Transcriptome analysis of the zebrafish *atoh7-/-* mutant, *lakritz*, highlights Atoh7-dependent genetic networks with potential implications for human eye diseases

Giuseppina Covello[1+], Fernando J. Rossello[2+], Michele Filosi[1+], Felipe Gajardo[3], Anne-Laure Duchemin[4], Beatrice F. Tremonti[1], Michael Eichenlaub[2], Jose M. Polo[2,6], David Powell[7], John Ngai[8], Miguel L. Allende[3], Enrico Domenici[1,4], Mirana Ramialison[2,*] and Lucia Poggi [1,4,9*]

[1] Department of Cellular, Computational and Integrative Biology - CIBIO, University of Trento, Italy

[2] Australian Regenerative Medicine Institute, Monash University Clayton VIC, Australia

[3] Center for Genome Regulation, Facultad de Ciencias, Universidad de Chile

[4] Centre for Organismal Study, Heidelberg University, Heidelberg, Germany

[5] Fondazione The Microsoft Research - University of Trento Centre for Computational and Systems Biology, Rovereto (Trento), Italy

[6] BDI, Monash University Clayton VIC, Australia

[7] Monash Bioinformatics Platform, Monash University Clayton VIC, Australia

[8] University of California, Department of Molecular and Cell Biology & Helen Wills Neuroscience Institute, Berkeley CA, USA

[9] Department of Physiology, Development and Neuroscience, University of Cambridge, Cambridge, United Kingdom

[+] G.Covello, F.J.Rossello and M.Filosi contributed equally to this work

[*] Correspondence should be addressed to:

L.P., Molecular and Cellular Ophthalmology Laboratory, Department of Cellular, Computational and Integrative Biology - CIBIO, University of Trento, Via Sommarive, 9, 38123, Trento, Italy. Tel. +390461283931; e-mail address: lucia.poggi@unitn.it.

M.R., Australian Regenerative Medicine Institute, Monash University, 15 Innovation Walk Clayton VIC, 3800, Australia. Tel.+61399029645. e-mail address: mirana.ramialison@monash.edu.

Current address:

Fernando Rossello: University of Melbourne Centre for Cancer Research, University of Melbourne, Melbourne, Victoria, Australia

Giuseppina Covello: Department of Biology, University of Padova, Padova, Italy

Short Running Title: Atoh7 genetic networks and human eye diseases.

Nonstandard Abbreviations:

RPCs: retinal progenitor cells

NCRNA: retinal non-attachment

ONH: optic nerve hypoplasia

ONA: optic nerve aplasia

PHPV: persistent hyperplastic primary vitreous

RGCs: retinal ganglion cells

EFTFs: eye field transcription factors

ABSTRACT:

Expression of the bHLH transcription protein Atoh7 is a crucial factor conferring competence to retinal progenitor cells for the development of retinal ganglion cells. A number of studies have emerged establishing *ATOH7* as a retinal disease gene. Remarkably, such studies uncovered *ATOH7* variants associated with global eye defects including optic nerve hypoplasia, microphthalmia, retinal vascular disorders and glaucoma. The complex genetic networks and cellular decisions arising downstream of *atoh7* expression, and how their dysregulation cause development of such disease traits remains unknown. To begin to understand such Atoh7-dependent events *in vivo* we performed transcriptome analysis of wild type and *atoh7* mutant (*lakritz*) zebrafish embryos at the onset of retinal ganglion cell differentiation. We investigated *in silico* interplays of *atoh7* and other disease-related genes and pathways. By network reconstruction analysis of differentially expressed genes we identified gene clusters enriched in retinal development, cell cycle, chromatin remodelling, stress response and Wnt pathways. By weighted gene coexpression network we identified coexpression modules affected by the mutation and enriched in retina development genes tightly connected to *atoh7*. We established the groundwork whereby Atoh7-linked cellular and molecular processes can be investigated in the dynamic multi-tissue environment of the developing normal and diseased vertebrate eye.

KEY WORDS: Atoh7, Ath5, retinal ganglion cells, transcriptome analysis; inherited eye diseases; human retina; zebrafish

INTRODUCTION

Retinal ganglion cells (RGCs) collect visual information from the neural retina in the eye and convey it to the visual cortex of the brain. In healthy people, this information is transmitted along the optic nerve, which is composed mainly of axons formed from the cell bodies of RGCs. Inherited diseases affecting the development of RGCs and the optic nerve can interrupt this information flow causing permanent blindness [1,2]. Atoh7 is an evolutionarily conserved, developmentally regulated transcription factor crucial for the genesis of RGCs in different vertebrate models [3–7]. Studies have shown that induced or naturally occurring mutations in the *atoh7* gene result in retinal progenitor cells (RPCs) failing to develop into RGCs and the optic nerve [3,5,6]. This occurs concomitantly with a comparable increase in the other main retinal cell types namely, amacrine, horizontal, bipolar, photoreceptor and Müller glial cells, suggesting a fate switch in the RPCs [3–6,8–11]. An increasing number of studies highlight *ATOH7* as an emerging candidate for eye diseases in humans. Variations in the *ATOH7* locus have been associated with optic nerve hypoplasia (ONH) and aplasia (ONA) [12–15], further pointing towards a crucial role of *atoh7* in RGC genesis and optic nerve development. Remarkably, a number of studies also have emerged, which highlight *ATOH7* variants as associated with multiple eye disease traits. For example, genome-wide association studies have reported *ATOH7* variants linked to glaucoma-related traits [16–23]. Likewise, multiple global eye developmental defects causing congenital blindness have been associated with mutations in *ATOH7*; these include autosomal recessive congenital disorders of the retinal vasculature, such as retinal non-attachment (NCRNA) and persistent hyperplastic primary vitreous (PHPV)(OMIM:# 221900, ORPHA:91495) [12,14,24–29] as well as corneal opacity, microcornea and microphthalmia (ORPHA:289499) [14,30]. Whilst the development of such global eye disorders might result from the association of variations in *ATOH7* and other genes [20,31,32], these findings suggest direct or indirect requirements of Atoh7 in multiple molecular and cellular interactions during ocular tissue development. For example, retinal vascular disorders likely result from the interruption of RGC development by the *ATOH7* mutations [13,28]. The Atoh7-regulated gene networks involved, and how their disruption contribute to the interruption of these retinal neural-vascular interactions remain unknown.

Given the well-established requirement of Atoh7 for RGC development in vertebrate models, several studies from different species have emerged to identify Atoh7-dependent gene batteries; which may also serve as instructive reprogramming factors to efficiently and irreversibly direct retinal progenitor or stem cells towards RGC differentiation pathways [7,33–42]. Whilst considerable progress has been made in this direction, whether Atoh7 is a master regulator instructing RGC differentiation programs remains debatable. For example, Atoh7 forced expression is often insufficient for bursting RGC fate commitment [42–44]. Investigators have also shown that, similarly to other bHLH factors in the developing central nervous system [45], *atoh7* expression levels are found in cycling retinal progenitor cells acquiring multiple retinal fates [8–10,46–49]. Concordantly, an increasing number of evidences suggest Atoh7-requirement in the control of retinal progenitor cell cycle progression as well as their competence and RGC identity acquisition [47,50–54]. Furthermore, *atoh7* expression is transient, being turned on just before the last mitotic division of RGC progenitors and downregulated shortly after the terminal division of the specified RGC daughter [8,48]. All of these observations call for the need of a deeper understanding as to the cell context- and *atoh7*-dependent regulatory networks that integrate multipotency, self-renewal, lineage-restriction, and cell-specific interactions immediately preceding and during RGC and optic nerve genesis. Also important is to investigate these networks *in vivo*, while observing integrated cell behaviours and vascular-neural interactions occurring in the physiological environment of the developing eye. This approach should inform on how, deregulation of key genes and molecular pathways might affect eye tissue development and interactions, thereby potentially contributing to the described *ATOH7*-associated global eye developmental disorders [55].

To this end, the zebrafish has long been valued as a paradigm for disentangling the genetics and cell biology of fundamental eye developmental processes [56,57]. The rapidly and externally developing transparent zebrafish embryos are amenable to easy genetic manipulation, thus allowing fast generation and identification of mutants modelling human ocular genetic disorders [58–64]. Such disease models can be concurrently investigated in large-scale genetics, drug screening, *in vivo* cell biology of early disease development as well as behavioural assays [65–68]. These potentials substantially aid fast progress in the validation of human genome association studies and in preclinical therapy development paths towards the early diagnosis and/or restoration of visual function [69–72].

We here begin to explore the potentials of the *lakritz* zebrafish mutant carrying a loss of function mutation in the *atoh7* gene [6] to investigate Atoh7-regulated gene networks and interrogate how deregulation of these networks during early onset of RGC genesis might contribute to the development of *atoh7*-associated eye disorders. With the analysis of available microarray data, we provide a cohort of statistically significantly regulated Atoh7 target genes, including previously known Atoh7-targets such as *atoh7* itself [33,53]. Remarkably, at this early RGC developmental time-point, the most significant targets comprehend previously unreported eye field transcription factors, Wnt signalling pathway components, chromatin and cytoskeletal regulators, and even stress-response proteins as major Atoh7-regulated genes. Interestingly, components of these pathways include eye disease gene markers.

With these data in hand, we can now begin to exploit the power of zebrafish as an *in vivo* vertebrate model to assess how dysregulation of one or more of these components might together affect the developing native ocular tissues. Understanding the cellular context and dynamics of these Atoh7-dependent networks will hopefully provide us with a next step forward in the identification of potential targets for the early detection and/or specific treatment of inherited eye diseases such as retinal-vascular disorders.

MATERIALS AND METHODS

Wild-Type and Transgenic Zebrafish

Fish used in this study were identified heterozygous carriers of the *lakritz* mutation [6] crossed in the (AB/AB) background as well as transgenic *tg(lakritz/atoh7:gap43-RFP)* heterozygous carriers [9,53]. All fish were maintained at 26-28°C and embryos raised at 28.5°C or 32°C and staged as described previously [73,74]. Embryos were obtained by breeding adult male and female fish at ratio 1:3. After fertilization, eggs were collected and maintained at 28.5°C and staged using standard morphological criteria [73]. Fish were kept and experiments were performed in accordance to local animal welfare agencies and European Union animal welfare guidelines.

Eyes and Body sample collection

Single pairs of eyes were dissected from single embryos at 25, 28, 35, 48, 72, and 96 hpf stages and snap-frozen in liquid nitrogen, and stored at −80 °C. Embryos older than 28 hpf were first

anesthetized for 5–10 min in Ethyl 3-aminobenzoate methanesulfonate (MS-222) (Sigma-Aldrich, Saint Louis, MO, USA) in E3 medium. The corresponding body of each embryo was collected and used immediately to perform genotyping analysis to identify the corresponding to *lakritz* and wild type eyes. All embryos were collected from the same batches of fish stock to maintain a uniform genetic background.

DNA extraction from zebrafish body biopsies and genotyping

Genomic DNA extraction from each single body was performed in 100 µl of lysis buffer containing Proteinase K-20mg/ml (EuroClone S.p.A. Milan, Italy), 2 M Tris-HCl ph 8.0, 0.5 M EDTA ph 8.0 and 5 M NaCl, 20 % SDS in a final volume of 50 µl ultra H_20. After 3 hours of incubation at 65°C, the gDNA was purified with an Ethanol precipitation step and resuspended in 50 µl of Dnase/Rnase H_2O. The genotyping was performed by Restriction Fragment Length Polymorphism (RFLP) assay as previously described [6]. An ~ 300 bp fragment of *atoh7* was PCR amplified with 1 U Taq DNA polymerase (Applied Biosystems by Life Technologies, Carlsbad, CA, USA) according to manufacturer protocols in a 30µl PCR mix containing 100ng of purified gDNA (from each single embryo body) with the following primers: Forward 5′ CCGGAATTACATCCCAAGAAC-3′ and Reverse 5′-GGCCATGATGTAGCTCAGAG-3′. The PCR conditions were as follows: initial denaturation (95°C for 5 minutes), followed by 40 cycles of denaturation (95°C for 45 seconds), annealing (56°C for 45 seconds), extension (72°C for45 second), and a final extension at 72 °C for 5 minutes. The resulting PCR product was digested with StuI restriction enzyme (NEB, New England Biolabs, Ipswich, MA, USA), according to manufacturer protocols. The digested product was analysed on a 2% agarose gel in 1X Tris-Acetate EDTA (TAE) buffer (Sigma-Aldrich, Saint Louis, MO, USA) to highlight wt or *lakritz* mutant corresponding fragments. The L44P mutation [6]eliminates a restriction site found in the published L44 allele The L44P mutation eliminates a restriction site found in the published L44 allele (Masai et al., 2000) and therefore can be visualised as an undigested ~ 300 bp fragment rather than the ~ 100 and ~ 200 bp fragments expected from the wt condition (**Fig. 1**). 1Kb DNA Ladder was used as a reference (Gene ruler 1Kb plus, Thermo Scientific, Carlsbad, CA, USA).

Affymetrix arrays hybridization and analysis

For the microarray analysis, 3 pairs of wt and *lakritz* 28-30 hpf embryos representing 3 biological replicates were dissected and placed in Trizol reagent (Thermo scientific Life Technologies, Carlsbad, CA, USA) for the total RNA extraction according to manufacturer's instructions. T7-based linear amplification of the mRNA was performed using the megascript kit from Ambion.

Hybridisation was performed on the Affymetrix GeneChip platform and processed according to standard procedure [75].

Correspondence between Zebrafish Affymetrix probesets and EnsEMBL gene annotations were retrieved using BioMart (EnsEMBL Version 84, March 2016) [76]. Batch effect removal was applied to adjust for known batch effect by first filtering the normalized matrix of intensities discarding probes with total abundance between samples lower than first quartile (Q1 = 16.26), and then correcting intensities using ComBat package [77] with extraction day as the known batch **(Supp. Fig. 1)**. Differential expression analysis between mutant and wild-type samples was performed using Limma package [78]For probes showing statistically significant differential expression (adj. P-value < 0.05), annotations of corresponding genes were retrieved from the EnsEMBL database using BiomaRt package [79].

Quantitative Real-Time PCR (qRT-PCR)

For the qRT-PCR analysis of *anillin* and *atoh7*, total RNA from five pulled pairs of frozen eyes, corresponding to either *lakritz* or wild type embryos, was used. After Turbo DNase treatment (Thermo scientific-Ambion, Carlsbad, CA, USA), according to manufacturer instructions, the RNA concentrations were measured with a Nanodrop ND-1000 spectrophotometer (NanoDrop Technologies Inc., Wilmington, USA). The RNA integrity was verified by loading the samples on 1% agarose gel that was run at 100 Volts in TBE 1X. 500 ng of extracted RNA from each sample was restrotrascribed with a RevertAidTM First Strand cDNA Synthesis Kit (Thermo SCIENTIFIC, Carlsbad, CA, USA), following manufacturer's protocol. Quantitative Real-time PCR reactions were performed on a Bio-Rad CFX96 Termo-cycler with Kapa Syber Fast qPCR master mix (2x) kit (Sigma-Aldrich, Saint Louis, MO, USA), according to the manufacturer's instructions. Templates were 1:10 diluted cDNA samples. For the negative controls cDNAs were replaced by DEPC water. All real-time assays were carried using 10ng of cDNA. The PCR profile was: 15 seconds at 95°C, followed by 40 cycles 60° C for 20 seconds, 72° C for 40 seconds. For the melting curve, 0.5°C was increased every 5 s from 65°C to 95 °C. All reactions were run in triplicate and both glyceraldehyde-3-phosphate dehydrogenase (GAPDH) and Ubiquitin Conjugating Enzyme E2 A (UBE2A) were used as reference genes. Each experiment was performed in triplicate and repeated two times. The relative gene expression was calculated using the ΔΔCT method. Statistical analyses were performed with Prism 5 (GraphPad Software, San Diego, CA), and statistical significance was set to $P<0.05$ for all experiments. The values are expressed as mean±SEM, and the

differences between groups were investigated using unpaired two-tailed Student t-test (GraphPad Software, San Diego, CA). A list of primers can be found in **Table 1**.

Table 1. List of primers with amplicon sizes used for quantitative Real-Time-PCR.

Primers	**Sequence (5' > 3')**	**Product length (bp)**
GAPHD_zf FOR	TCACAAACGAGGACACAACCA	219
GAPHD_zf REV	CGCCTTCTGCCTTAACCTCA	
Ube2a_zf FOR	CTGAAGGAACACCTTTTGAAGATG	215
Ube2a_zf REV	GATCCAGTAAAGACTGTATTGAG	
Atoh7_zf FOR	TCACCTGTGGAAAGTGACTG	254
Atoh7_zf REV	CTCATTCACAACCCGCCCAA	
Anln_zf FOR	AAAGGCTTCCTGACTATGTTTG	107
Anln_zf REV	CATCATCAGGGTAGGTCCA	

Functional category enrichment analysis and network analysis

Functional enrichment analysis was performed with Metascape [80] using the Danio rerio EnsEMBL IDs of the list of differentially regulated genes as "Input as species" and "Analysis as species" species through the custom analysis mode**.** Enrichment analysis was performed against GO "Biological Process" using P Value cutoff of 0.05 and otherwise default parameters. Human disease annotation was performed with Metascape using *Danio rerio* as "Input as species" and *H. sapiens* as "Analysis as species". Under the "Annotation" mode, all repositories under Genotype/Phenotype/Disease were selected for disease annotation. To rule out potential sampling or biological bias, we performed an additional enrichment analysis by restricting the background to the list of expressed genes as detected by the arrays, using both Metascape and KOBAS [81]. Network interactions between the differentially expressed genes were retrieved through the STRING database [82], "multiple proteins" mode and default parameters otherwise. Network interactions were visualised using Cytoscape [83]

Weighted Gene Co-expression Network Analysis

The pipeline proposed by Langfelder and collaborators [84] in their CRAN package was followed to infer gene co-expression networks and identify network modules within R 3.6.3 statistical environment. Networks were inferred using the TOMsimilarityFromExpr function with "cor" as gene coexpression measure. The soft-threshold parameter was optimized with the function pickSoftThreshold and the best threshold (α=16) selected by visual inspection in order to follow a scale-free topology model, as suggested by the WGCNA pipeline. Correlations between modules eigengenes, status and library batch were computed. Modules with the highest correlation for status and significant p-value (α<=0.05) were selected for further analysis. Within the selected modules, highly connected structure of submodules were identified using the leading eigenvector community detection method [85] implemented in the igraph package (v1.2.5) for R (http://igraph.com).

Whole mount Immunohistochemistry

For immunohistochemical labeling, embryos were fixed in 4 % PFA for 1 hour at room temperature or overnight at 4ºC. Embryos were washed 3 times in PTw and kept for a week maximum in PTw. Fixed embryos were blocked in blocking solution (10 % goat serum, 1 % bovine serum albumin, 0.2 % Triton X-100 in PBS) for one hour. Embryos were permeabilized with 0.25 % trypsin-EDTA (1X, Phenol red, Gibco – Life Technologies) on ice for 5 min. Primary (mouse anti-β-catenin, 1:100, BD Biosciences Cat. No 610153) and secondary (anti-mouse IgG conjugated to Alexa Fluor 488, 1:250, Invitrogen) antibodies were added for 2 overnights each and DAPI was added from the first day of incubation in the antibody mix. Stained embryos were kept in PTw at 4ºC in dark until imaging. Embryos were embedded onto a 35 mm Glass-bottom Microwell dish (p35G-1.5-10-C, MatTek) and oriented with a femtoloader tip (eppendorf) in the position needed for imaging until the agarose had polymerized. Confocal imaging was performed using a laser scanning confocal microscope Leica SpE using a Leica 40X, 1.15 NA oil-immersion objective.

For the analysis of the intensity along the apical-to-basal membrane, a line of a defined length along the apical-to-basal membrane was drawn for 9 cells at 3 different z-sections for each embryo. Signal intensities were obtained using Fiji and average values for the 9 cells were calculated. For the analysis of the intensity along the apical membrane, the number of peaks were counted after Ctnnb1 signal intensity measurement. For the signal intensity measurements, a line of defined length was drawn along the apical membrane of the retina on Fiji and signal intensities were retrieved. The length of line was the same for all z-sections of an individual embryo. Normalization

was performed by the highest value for each line . Measurements were obtained on 3 different z sections for each embryo.

RESULTS

Transcriptome analysis of wild type and *lakritz* identified 137 statistically significant differentially expressed genes

Expression of *atoh7* in the retina is first detected at around 25-28 hpf and it reaches its peak at around 36 hpf [86]. The earliest post-mitotic RGCs in the retina are detected at around 28 hpf, a developmental time-point corresponding to the earliest onset of retinal differentiation [87]. To identify early Atoh7-regulated genes, transcriptome analysis was performed on eyes from single *lak*$^{-/-}$ mutant (*lakritz*) [6] and wild type zebrafish embryos at 28-30 hours post fertilization (hpf) based on Affymetrix microarrays (see methods and **Fig. 1**).

Differential gene expression analysis performed with LIMMA resulted, after batch effect removal, with 171 significantly differentially expressed probes (adj. P-value < 0.05) (**Fig. 2A**) corresponding to 137 genes annotated onto EnsEMBL database (**Fig. 2B and Supplemental Table 1**). Among these, we confirmed down-regulation of *atoh7* in the *lakritz*, consistent with its known role as self-activator [33]. Also consistent with the presence of *bona fide* Atoh7-regulated targets in the 137 cohort is the presence of additional 7 genes, which have been previously reported to contain a well-characterised Ath5 consensus binding site [33,53]. Among the 8 Atoh7-direct targets, besides *atoh7* itself, the thyrotroph embryonic factor *tefa* [88] and the atypical cadherin receptor 1 *celsr1a (CELSR1)* [89] were down-regulated in the *lakritz*, suggesting their positive regulation by Atoh7. Conversely, the retina and anterior neural fold homeobox transcription factor *rx1 (RAX)* [90] the Wnt signalling pathway regulator *notum* [91] the transmembrane protein *tmem165* [92] and the F-actin binding protein and cytokinesis regulator *anillin (ANLN)* [93], were upregulated in the *lakritz*, suggesting that they are negatively modulated by Atoh7.

Functional category enrichment reveals neural retina, cell cycle and Wnt pathways regulated downstream of Atoh7

Functional enrichment analysis in Metascape using default parameters reveals "neural retina development" (GO:0003407) as the most highly significantly enriched GO Biological Process category, consistent with the role of Atoh7 as regulator of retinal development **(Fig. 3A and Supplemental Table 2)**. To further increase stringency, ruling out sampling or biological bias in the analysis, the background was restricted to the list of expressed genes as detected by the arrays [81] both using Metascape and Kobas 3.0, which incorporates knowledge from 5 pathway databases (KEGG PATHWAY, PID, BioCyc, Reactome and Panther), and 5 human disease databases (OMIM, KEGG DISEASE, FunDO, GAD and NHGRI GWAS Catalog). This analysis consistently underscored "neural retina development" (GO:0003407) as the enriched term both by Metascape (not shown) and Kobas (**Supplemental Table 3**). This category contains 9 statistically significantly differentially expressed genes (including *atoh7*), which comprehend early expressed eye-field transcription factors (EFTFs, *rx1* and *six6a*) [94–97], stress response and extracellular matrix remodelling factors (*hsp70.1*, *mmp14a*) [98–101], chromatin regulators (*smarca5*) [102] as well as microtubules organisers and cell cycle regulatory proteins (*tubgcp4*, *znf503*, *gnl2*) [103–105]. Other (albeit less significant) relevant biological processes emerging from this analysis were "cell cycle process" (GO:0022402), "chromatin remodeling" (GO:0006338) and "Wnt signaling pathway" (GO:0016055) (**Fig. 3B and Supplemental Table 2)**.

We next investigated the known relationships amongst the 137 Atoh7-regulated genes via network reconstruction analysis (see methods). Analysis conducted with STRING-DB v 11.0 s highlighted three main gene subnetworks, which are suggestive of the over-represented GO Biological processes, namely "retinal development", "cell cycle" and "Wnt signalling pathway" **(Fig. 4)**. Furthermore, this analysis suggested *atoh7, rx1 and six6a* as the core of a retinal "kernel" composed of early developmental eye-specific transcription factors [106] **(Fig. 4)**.

Weighted Gene Co-expression Network Analysis revealed a coexpression module with a cluster of genes tightly interconnected to Atoh7

To explore global changes of gene expression in the *lakritz* mutant, we conducetd a weight gene co-expression network analysis (WGCNA) [84] to the available microarray data. Notwithstanding the small number of samples, we identified 16 recurrent functional modules based on co-expression pattern analysis on the full transcriptome dataset. In order to identify co-expression modules significantly affected by the *lakritz* mutation, we tested for their association with available covariates, including batch and mutation status. Out of the 16 modules found, two of them showed a high correlation with the mutation condition (wild type vs *lakritz*). Specifically, modules 13 (overall

up regulated) and module 3 (overall down regulated) were found highly significant – with a correlation of 0.97 (p=0.002) and -0.99 (p=1e-5), respectively (**Supp. Fig. 2 and Supplemental Table 4**). Functional network analysis by STRING DB (https://string-db.org/cgi/network.pl?taskId=hNkdhEXQnBhR) on M13 (the smallest module, which we also found to contain *atoh7*) revealed an enrichment in "eye morphogenesis (blue color in **Supp. Fig. 3**), "retina layer formation" (red color in **Supp. Fig. 3**), and a cluster of genes previously found to be dysregulated in "light responsive, circadian rhythm processes" (PMID: 20830285 and PMID: 21390203) (light and dark green color in **Supp. Fig. 3**).

Lastly, we analyzed in detail the topology of the Module 13. We identified 4 submodules with high within-community connectivity, which show decreasing degree of connectivity from left to right **(Fig. 5).** The submodule containing *atoh7* (left) shows a densely interconnected cluster of genes with high topological overlap. These genes likely participate in common regulatory and signaling circuits including retina layer formation (e.g. *atoh7, rx1*) and Wnt/β-catenin signalling pathway (e.g. *fxd7a, tcf7l1b*).

DISCUSSION

Our differential gene expression analysis of transcriptome data revealed 137 genes that are significantly differentially expressed between *lakritz* and wild type eyes from embryos at a developmental time-point corresponding to the onset of RGC differentiation. We also applied multiple bioinformatics pipelines to perform a functional classification and network reconstruction of the differentially expressed genes. Notably, all methods here applied consistently highlighted "neural retina development" (GO:0003407) as the most biological pathway differentially affected by the *lakritz* mutation. Likewise, the interplay *atoh7*, *rx1* end *six6a* – early developmentally regulated EFTs – consistently emerged as the "kernel" network of this cluster.

The homebox transcription factor Rx1 is well known for its evolutionarily conserved role in the generation and maintenance of multipotent RPCs during morphogenesis and differentiation of the vertebrate eye [95,97,107–110]. Mutant variants of *RAX* family genes have been linked to congenital developmental eye disorders, particularly microphthalmia, further confirming an early requirement for RPC proliferation and stemness [29,111–113]. Based on these findings, the data from our analysis

suggest that balancing RPCs competence and RGC fate commitment requires *rx1* downregulation by Atoh7. Notably, Atoh7-mediated downregulation of *rx1* is likely direct, since previous *in silico* analyses highlighted the presence of an Atoh7-binding motive in the *rx1* gene cis-regulatory regions [33].

Conversely, *six6* genes have been reported as RPCs competence factors, on the one hand suppressing stemness and proliferation via Wnt/β-catenin signalling downregulation, on the other hand promoting expression of RGC differentiation genes [94]. These findings are in agreement with the present study reporting *six6a* being an Atoh7-upregulated gene. Remarkably variant forms of *SIX6 (SIX9/OPTX2)* have been linked to congenital microphthalmia as well as to the development of glaucoma [20,29,32,114–119]. Given that mutations in *ATOH7* have been also associated with similar global eye disorders [14,120], these observations strongly point at the importance to further understand the interplay *ATOH7*, *RX1* and *SIX6* during eye development, and to assess how disruption of this evolutionarily conserved genetic network might be linked to such eye disorders [121].

Besides *atoh7*, *rx1* and *six6a,* significant differentially expressed genes annotated with "neural retina development" were *tubgcp4*, *gnl2*, *smarca5*, *mmp14a*, *znf503*, and *hsp70.1*. The Atoh7-upregulated gamma-tubulin complex protein 4 encoding gene *tubgcp4* is of great interest. Variants of *TUBGCP4* have been linked to autosomal-recessive microcephaly with chorioretinopathy, which comprise a spectrum of eye developmental anomalies including microphthalmia, optic nerve hypoplasia, retinal folds, and absence of retinal vasculature [103]. This raises the possibility that regulation of this gene might link Atoh7 to retinal-vascular development as well as retinal neurogenesis. Genetic evidences for the GTPase and zinc finger transcriptional repressor encoding genes, *gnl2* and *znf503 (NOLZ1)* as eye disorders-related genes are still missing but studies support their functional requirement for retinal developmental processes, including proper cell cycle exit of RPCs during RGC differentiation [104,105]. Notably, *tubgcp4* and *gnl2* and *znf503* were implicated in the regulation of cytokinesis late in mitosis [103–105]. This observation further indicates Atoh7-requirements for the regulation of cell cycle progression, at least in RPCs. The SWI/SNF chromatin remodelling factors have been reported as crucial regulators of the transition from multipotent to committed progenitor and differentiated cell states in multiple eye tissues, with potential implications for eye disorders [122–125]. The finding of *smarca5* as an upregulated gene in the *lakritz* indicates the importance to address functional implications of this gene for *atoh7*-related eye disorders. Furthermore, the "neural retina development" Gene Ontology category encompassed the reportedly stress response genes *hsp70.1(HSPA1L)* [101] and *mmp14* [126] as significantly differentially

down- and up- regulated, respectively, by the *lakritz* mutation. The crystallin related, heat shock Hsp70 family proteins are emerging as important regulators of RGC survival and regeneration as well as retinal vascular remodelling factors [101,127–129]. The intriguing finding that *hsp70.1* is highly enriched among the Atoh7-upregulated genes in the "neural retina development" gene cluster supports the idea that upregulation of these stress-response proteins might be relevant also during RGC development. Lastly, the extracellular matrix remodelling factor Mmp14 is reportedly a crucial regulator of cell stemness and vascular remodelling [130]. Studies have also implicated Mmp14a in retinal developmental processes such as RGC axon guidance and innervation of the optic tectum [98–100]. Future studies will assess the functional implication of Atoh7-mediated downregulation of *mmp14a* during vascular-retinal development. Interestingly, our network analysis reveals that *mmp14a* is linked with known components of the Wnt signalling pathway, further underscoring the importance of the interplay of this pathway and Atoh7.

The "Wnt signalling pathway" is the second Atoh7-dependent subnetwork emerging in our functional network analysis; which is centered around the *ctnnb1* (β-catenin) gene **(Fig. 4).** Studies have shown that the Wnt/β-catenin pathway promotes RPC proliferation and stemness whilst suppressing *atoh7* activation and RGC differentiation [131–133]. We here find that the main differentially expressed components of this pathway, namely *ctnnb1*, *fxd7a* and *tcf7l1b*, are upregulated in the *lakritz* mutant, suggesting Atoh7 requirement in the Wnt/β-catenin pathway downregulation **(Fig. 4)**. Concordantly, studies have reported that *atoh7*-expressing retinal progenitors contain low levels of expression in Wnt/β-catenin pathway components when compared with non-*atoh7*-expressing progenitor cells [35] further suggestive of a negative feedback regulatory loop integrating Atoh7 and Wnt/β-catenin signalling. Conversely, the planar cell polarity (PCP) signalling component *celsr1a/flamingo*, which has been reported as key regulator of neuronal cell differentiation, neurite outgrowth and axon guidance [134] emerges as an Atoh7-upregulated gene in our cohort. A number of studies reported dysregulation of Wnt signalling being associated with retinal diseases [133,135–137]. Likewise, Wnt, Fzd7/β-catenin pathway has been reported as an important modulator of retinal vascular remodelling [138]. Further research will clarify the genetic regulatory networks integrating Atoh7 and Wnt/β-catenin signaling in controlling multiple eye tissue development in the vertebrate, and how their dysregulation might results in multiple ocular disorders [139].

Previous studies highlighted the importance of the interplay of Atoh7 with components of the Notch signalling pathway for RGC development and regeneration [43,50,140]. In particular, downregulation of Notch signalling pathway has been proposed as a general mechanism whereby RGC genesis can be

enhanced [140–143]. According to these findings, Notch pathway components (*hes6*, *mib1*, *hdac*, *adam17b*, and *Notch1a*) appear affected by the *lakritz* mutation in our gene expression microarray data **(Supplementary Table 1)** but their expression does not change significantly between wild type and *lakritz* condition in our analysis **(Supplementary Table 1)**. However, even though they fail short of the significance threshold of adjusted p-value < 0.05, it is worth noting that their values suggest a trend in downregulation of Notch pathway-related genes **(Supplementary Table 1).** We suppose that such lack of significance in the differential expression might be linked to the developmental stage used for this analysis. Likewise, the extracted cohort of significantly regulated genes does not comprehend some of the reported RGC maturation-associated factors, such as Cxcr4b, Elavl3 and Isl1 [33,35,37,53]. Nonetheless, for *cxcr4b* and *elavl3a*, -1.43 FC (nominal p-value of 0.0018) and -1.39 FC (nominal p-value 0.0066) was observed, respectively, consistently with a positive regulation by Atoh7 (downregulated in the *lakritz*). We therefore suppose that expression of such RGC maturation-related factors downstream of Atoh7 might be too low at the developmental time-point selected for this study, to be detected within the chosen significance range.

In support of the Atoh7-dependent transcriptional regulation of progenitor cell division and developmental progression, a third Atoh7-dependent subnetwork emerged in our functional network analyses, which includes cell-cycle and chromatin regulators **(Fig. 4)**. One *bona fide* gene of great interest in this subnetwork is the F-actin binding and cytokinesis regulator Anillin (*ANLN*) [53,144,145]. Anillin has attracted increasing attention as a potential disease-related gene (ORPH:93213, OMIM:616027). Evidence point at *anillin* expression levels being associated with cell proliferation and migration disorders in cancer and kidney diseases [146–149]. Additional roles for this actin binding protein have been reported in nerve cell development [150,151] and dysregulation of Anillin has been implicated in central nervous system myelin disorders [152,153]. In the zebrafish retina, *anillin* expression levels appears required to favour cell cycle progression and restrict RGC genesis in Atoh7-expressing RPCs [53]. Concordantly, in the presence of *anillin* downregulation many more RPCs turn on *atoh7* and become RGCs [53]. We here find *anillin* as an Atoh7-downregulated gene, suggesting that a molecular feedback regulatory loop of an as yet unknown nature between *anillin* and *atoh7* is at work, to balance RPCs developmental progression. Whilst further investigations will address this question, the functional network analyses from this study suggest that the Wnt/β-catenin signalling pathway might be involved. Studies have shown that *anillin* expression is positively associated with the expression of β-catenin (*ctnnb1*) [154] consistent with *ctnnb1* also being an Atoh7-downregulated gene in our gene cohort. Furthermore, Anillin appears to be an essential

regulator of epithelial cell-cell adherens junctions via regulation of the E-Cadherin/β-catenin complex [148,155,156]. In agreement with this idea, we here make the preliminary observation that *anillin* knock down results in accumulation and displacement of β-catenin signal in the apical and apical-lateral membrane of RPCs **(Supp. Fig. 4A,B)**. Notably, in addition to promoting cell-to-cell adhesion [157,158] β-catenin functions as nuclear transcriptional co-activator of Wnt signalling responsive genes promoting proliferation and inhibiting differentiation [159–161]. Thus, regulation of β-catenin accumulation and localization to the E-Cadherin/β-catenin complex might be a mechanism whereby Anillin controls not only cell adhesion dynamics, but also Wnt signalling pathway activity [157]. It is also intriguing to note that high levels of *anillin* expression where found in human choroidal endothelial cells, leading to the obvious hypothesis that Anillin is a potential regulator of choroidal angiogenesis [162,163]. These observations suggest both RPCs and endothelial cell behaviours might require *anillin* expression levels during retinal-vascular developmental interactions. Future studies will assess the functional implications of the interplay of Atoh7, Anillin and Wnt pathway components for the dysregulation of eye developmental processes. In line with this hypothesis is our preliminary observation that *anillin* remains significantly affected (namely upregulated) by the *lakritz* condition, starting from 25 hpf (coinciding with the onset of *atoh7* expression [86]) until after 72 hpf (when all retinal layers are fully differentiated [87]). Furthermore, the extent of such upregulation in subsequent developmental stages suggests oscillatory dynamics of *anillin* transcriptional downregulation by Atoh7 **(Supp. Fig. 4C)**. Overall, these observations further underscore the importance of feedback loops involving Atoh7, *anillin* and Wnt signalling, the dysregulation of which could possibly contribute to the development of vascular-retinal disorders.

Finally, we have applied weighted gene co-expression network analysis to explore gene co-expression relationships and identify co-expression modules potentially involved in *atoh7* function. In addition to highlighting the already known interaction networks that were enriched within the 137 differentially regulated genes, we were able to identify two co-expression modules significantly affected by the *lakritz* mutation (**Supplementary Table 4**). One of them in particular (module 13) contains a cluster of highly interconnected genes including *atoh7* itself, *rx1* and members of the Wnt signalling pathway (e.g. *tcf7l1b*, *fzd7a* and *mmp14a)*. This analysis therefore further confirms tight functional interaction between neural retinal development and Wnt pathway genes from our gene differential expression data.

Lastly, our knowledge-based analysis of the M13 members by STRING database further extended these finding by revealing the existence of a network of interactions between *atoh7* and *rx1* dependent "retina layer formation", "eye morphogenesis" pathways, Wnt signalling pathway components (e.g. *tcf7l1b*, *fzd7a* and *mmp14a)*, and two new gene networks previously found to be dysregulated in light responsive, circadian rhythm processes [88,164] **(Supp. Fig. 3)** (https://string-db.org/cgi/network.pl?taskId=hNkdhEXQnBhR). At present, very little is known on the functional importance of circadian clock genes, but increasing evidence indicates their implication in multiple eye tissues developmental processes as well as ocular disorders [165–169]. This study further supports this evidence, by showing that Atoh7-dependent regulatory networks integrates such circadian clock genes.

In sum, this Atoh7 targets analysis extends data from other studies focussing on transcription factors cascades enhancing RGC differentiation. We here provide new insights on Atoh7-dependent developmental processes that might be regulated in global developmental eye disorders. First, they suggest that Atoh7 directly controls a two-tiered regulatory network balancing early acquisition of progenitor cell competence (*e.g.* through *six6a*, *rx1*) and repression of pro-multipotency and proliferative processes (*e.g.* through chromatin remodelling, cell cycle and Wnt pathway regulation). Secondly, these data highlight for the first time many previously unreported cytoskeletal proteins, chromatin remodelling factors, stress-response proteins, and even circadian clock genes as Atoh7-regulated genes. Third, this analysis underscores both direct and potential functional genetic links of many of these factors to eye developmental disorders. This study thus contributes to laying the groundwork for the identification of key candidate molecules and their networks as potential targets for early eye disease detection and therapeutic applications.

ACKNOWLEDGEMENTS

We are grateful to W.A. Harris for supporting this study at Cambridge University and Karen Vranizan (University of California) for technical assistance. We also thank I. Pradel and F. Zolessi (University of Cambridge) for technical assistance and F. Zolessi for discussion. We acknowledge S. Sel (University of Heidelberg) for material support. We thank the fish facility management group for fish maintenance and technical assistance. This work was supported by the Wellcome Trust, the Deutsche Forschungsgemeinschaft Research Grant PO 1440/1-1 to L. Poggi, the Landesgraduiertenförderung (Funding program of the State of Baden Württemberg, Germany) to A-L. Duchemin and the Australian Research Council Discovery Project Grants DP140101067 and

DP190102771 to M. Ramialison. The Australian Regenerative Medicine Institute is supported by grants from the State Government of Victoria and the Australian Government. M. L. Allende and F. Gajardo were supported by ANID/FONDAP/15090007; F. Gajardo acknowledges the support of CONICYT REDES 150094.

AUTHOR CONTRIBUTIONS

L. Poggi designed research; G. Covello, A-L Duchemin, F.B. Tremonti, L. Poggi and J.Ngai performed experiments; F.J. Rossello, M. Filosi, F. Gajardo, E. Domenici, M. Eichenlaub, M. Ramialison performed bioinformatic analysis with inputs from J.M. Polo, D. Powell, M. L. Allende; L. Poggi and M. Ramialison wrote the manuscript with inputs from all authors.

REFERENCES

1. Zeki, S. M. & Dutton, G. N. Optic nerve hypoplasia in children. *Br. J. Ophthalmol.* (1990).
2. Dutton, G. N. Congenital disorders of the optic nerve: Excavations and hypoplasia. *Eye* (2004). doi:10.1038/sj.eye.6701545
3. Brown, N. L., Patel, S., Brzezinski, J. & Glaser, T. Math5 is required for retinal ganglion cell and optic nerve formation. *Development* **128**, 2497–2508 (2001).
4. Kanekar, S. *et al.* Xath5 participates in a network of bHLH genes in the developing xenopus retina. *Neuron* (1997). doi:10.1016/S0896-6273(00)80391-8
5. Wang, S. W. *et al.* Requirement for math5 in the development of retinal ganglion cells. *Genes Dev.* (2001). doi:10.1101/gad.855301
6. Kay, J. N., Finger-Baier, K. C., Roeser, T., Staub, W. & Baier, H. Retinal Ganglion Cell Genesis Requires lakritz, a Zebrafish atonal Homolog. *Neuron* **30**, 725–736 (2001).
7. Sapkota, D., Wu, F. & Mu, X. Focus on Molecules: Math5 and retinal ganglion cells. *Exp. Eye Res.* **93**, 796–797 (2011).
8. Brzezinski, J. A., Prasov, L. & Glaser, T. Math5 defines the ganglion cell competence state in a subpopulation of retinal progenitor cells exiting the cell cycle. *Dev. Biol.* **365**, 395–413 (2012).
9. Jusuf, P. R. *et al.* Biasing amacrine subtypes in the Atoh7 lineage through expression of barhl2. *J. Neurosci.* **32**, 13929–13944 (2012).
10. Poggi, L., Vitorino, M., Masai, I. & Harris, W. A. Influences on neural lineage and mode of

division in the zebrafish retina in vivo. *J. Cell Biol.* **171**, 991–999 (2005).

11. Jusuf, P. R. *et al.* Origin and determination of inhibitory cell lineages in the vertebrate retina. *J. Neurosci.* **31**, 2549–2562 (2011).
12. Brown, N. L., Dagenais, S. L., Chen, C. M. & Glaser, T. Molecular characterization and mapping of ATOH7, a human atonal homolog with a predicted role in retinal ganglion cell development. *Mamm. Genome* **13**, 95–101 (2002).
13. Atac, D. G. *et al.* Atonal homolog 7 (ATOH7) loss-of-function mutations in predominant bilateral optic nerve hypoplasia. *Hum. Mol. Genet.* (2019). doi:10.1093/hmg/ddz268
14. Khan, K. *et al.* Next generation sequencing identifies mutations in atonal homolog 7 (ATOH7) in families with global eye developmental defects. *Hum. Mol. Genet.* (2012). doi:10.1093/hmg/ddr509
15. Lim, S. H. *et al.* Sequencing analysis of the ATOH7 gene in individuals with optic nerve hypoplasia. *Ophthalmic Genet.* (2014). doi:10.3109/13816810.2012.752017
16. Chen, J. H. *et al.* Interactive effects of ATOH7 and RFTN1 in association with adult-onset primary open-angle glaucoma. *Investig. Ophthalmol. Vis. Sci.* (2012). doi:10.1167/iovs.11-8277
17. Fan, B. J., Wang, D. Y., Pasquale, L. R., Haines, J. L. & Wiggs, J. L. Genetic variants associated with optic nerve vertical cup-to-disc ratio are risk factors for primary open angle glaucoma in a US Caucasian population. *Investig. Ophthalmol. Vis. Sci.* **52**, 1788 (2011).
18. Macgregor, S. *et al.* Genome-wide association identifies ATOH7 as a major gene determining human optic disc size. *Hum. Mol. Genet.* **19**, 2716–2724 (2010).
19. Micheal, S. *et al.* Association of known common genetic variants with primary open angle, primary angle closure, and pseudoexfoliation glaucoma in Pakistani cohorts. *Mol. Vis.* **20**, 1471–9 (2014).
20. Philomenadin, F. S. *et al.* Genetic Association of SNPs near ATOH7, CARD10, CDKN2B, CDC7 and SIX1/SIX6 with the Endophenotypes of Primary Open Angle Glaucoma in Indian Population. *PLoS One* **10**, e0119703 (2015).
21. Ramdas, W. D. *et al.* Clinical Implications of Old and New Genes for Open-Angle Glaucoma. *Ophthalmology* **118**, 2389–2397 (2011).
22. Springelkamp, H. *et al.* An international genome-wide association study of glaucoma-related optic disc parameters in 18,000 caucasians: The international glaucoma genetics consortium. *Investig. Ophthalmol. Vis. Sci.* (2013).
23. Venturini, C. *et al.* Clarifying the role of ATOH7 in glaucoma endophenotypes. *Br. J. Ophthalmol.* **98**, 562–566 (2014).

24. Garcia-Montalvo, I. A. *et al.* Mutational screening of FOXE3, GDF3, ATOH7, and ALDH1A3 in congenital ocular malformations. Possible contribution of the FOXE3 p.VAL201MET Variant to the risk of severe eye malformations. *Ophthalmic Genetics* (2014). doi:10.3109/13816810.2014.903983

25. Ghiasvand, N. M. *et al.* Deletion of a remote enhancer near ATOH7 disrupts retinal neurogenesis, causing NCRNA disease. *Nat. Neurosci.* **14**, 578–586 (2011).

26. Khor, C. C. *et al.* Genome-wide association studies in Asians confirm the involvement of ATOH7 and TGFBR3, and further identify CARD10 as a novel locus influencing optic discarea. *Hum. Mol. Genet.* (2011). doi:10.1093/hmg/ddr060

27. Kondo, H., Matsushita, I., Tahira, T., Uchio, E. & Kusaka, S. Mutations in ATOH7 gene in patients with nonsyndromic congenital retinal nonattachment and familial exudative vitreoretinopathy. *Ophthalmic Genetics* **37**, 462–464 (2016).

28. Prasov, L. *et al.* ATOH7 mutations cause autosomal recessive persistent hyperplasia of the primary vitreous. *Hum. Mol. Genet.* **21**, 3681–3694 (2012).

29. Wright, C. F. *et al.* Genetic diagnosis of developmental disorders in the DDD study: A scalable analysis of genome-wide research data. *Lancet* (2015). doi:10.1016/S0140-6736(14)61705-0

30. Khan, K. *et al.* Genetic heterogeneity for recessively inherited congenital cataract microcornea with corneal opacity. *Investig. Ophthalmol. Vis. Sci.* (2011). doi:10.1167/iovs.10-6776

31. Wang, D. G., Chen, J. H., Zhang, M. Z. & Zheng, Y. Q. Interactive effects of ATOH7 and RFTN1 in association with juvenile primary open-angle glaucoma. *Int. Eye Sci.* **17**, 440–443 (2017).

32. Abu-Amero, K., Kondkar, A. & Chalam, K. An Updated Review on the Genetics of Primary Open Angle Glaucoma. *Int. J. Mol. Sci.* **16**, 28886–28911 (2015).

33. Del Bene, F. *et al.* In vivo validation of a computationally predicted conserved Ath5 target gene set. *PLoS Genet.* **3**, 1661–1671 (2007).

34. Mu, X. & Klein, W. H. A gene regulatory hierarchy for retinal ganglion cell specification and differentiation. *Seminars in Cell and Developmental Biology* (2004). doi:10.1016/j.semcdb.2003.09.009

35. Gao, Z., Mao, C.-A., Pan, P., Mu, X. & Klein, W. H. Transcriptome of Atoh7 retinal progenitor cells identifies new Atoh7 -dependent regulatory genes for retinal ganglion cell formation. *Dev. Neurobiol.* **74**, 1123–1140 (2014).

36. Mu, X. *et al.* A gene network downstream of transcription factor Math5 regulates retinal

progenitor cell competence and ganglion cell fate. *Dev. Biol.* **280**, 467–481 (2005).

37. Wu, F. *et al.* Two transcription factors, Pou4f2 and Isl1, are sufficient to specify the retinal ganglion cell fate. *Proc. Natl. Acad. Sci. U. S. A.* (2015). doi:10.1073/pnas.1421535112
38. Poggi, L., Vottari, T., Barsacchi, G., Wittbrodt, J. & Vignali, R. The homeobox gene Xbh1 cooperates with proneural genes to specify ganglion cell fate within the Xenopus neural retina. *Development* **131**, 2305–2315 (2004).
39. Pacal, M. & Bremner, R. Induction of the ganglion cell differentiation program in human retinal progenitors before cell cycle exit. *Dev. Dyn.* (2014). doi:10.1002/dvdy.24103
40. Song, W. T., Zhang, X. Y. & Xia, X. B. Atoh7 promotes the differentiation of retinal stem cells derived from Müller cells into retinal ganglion cells by inhibiting Notch signaling. *Stem Cell Res. Ther.* (2013). doi:10.1186/scrt305
41. Song, W. tao, Zhang, X. yong & Xia, X. bo. Atoh7 promotes the differentiation of Müller cells-derived retinal stem cells into retinal ganglion cells in a rat model of glaucoma. *Exp. Biol. Med.* (2015). doi:10.1177/1535370214560965
42. Prasov, L. & Glaser, T. Pushing the envelope of retinal ganglion cell genesis: Context dependent function of Math5 (Atoh7). *Dev. Biol.* (2012). doi:10.1016/j.ydbio.2012.05.005
43. Song, W. tao, Zeng, Q., Xia, X. bo, Xia, K. & Pan, Q. Atoh7 promotes retinal Müller cell differentiation into retinal ganglion cells. *Cytotechnology* (2016). doi:10.1007/s10616-014-9777-1
44. Sinn, R., Peravali, R., Heermann, S. & Wittbrodt, J. Differential responsiveness of distinct retinal domains to Atoh7. *Mech. Dev.* (2014). doi:10.1016/j.mod.2014.08.002
45. Kageyama, R., Shimojo, H. & Ohtsuka, T. Dynamic control of neural stem cells by bHLH factors. *Neuroscience Research* (2019). doi:10.1016/j.neures.2018.09.005
46. Feng, L. *et al.* MATH5 controls the acquisition of multiple retinal cell fates. *Mol. Brain* (2010). doi:10.1186/1756-6606-3-36
47. Lust, K., Sinn, R., Pérez Saturnino, A., Centanin, L. & Wittbrodt, J. De novo neurogenesis by targeted expression of atoh7 to Müller glia cells. *Dev.* (2016). doi:10.1242/dev.135905
48. Miesfeld, J. B., Glaser, T. & Brown, N. L. The dynamics of native Atoh7 protein expression during mouse retinal histogenesis, revealed with a new antibody. *Gene Expr. Patterns* **27**, 114–121 (2018).
49. Yang, Z., Ding, K., Pan, L., Deng, M. & Gan, L. Math5 determines the competence state of retinal ganglion cell progenitors. *Dev. Biol.* (2003). doi:10.1016/j.ydbio.2003.08.005
50. Chiodini, F. *et al.* A Positive Feedback Loop between ATOH7 and a Notch Effector Regulates Cell-Cycle Progression and Neurogenesis in the Retina. *Cell Rep.* **3**, 796–807

(2013).

51. Dvoriantchikova, G. *et al.* Molecular Characterization of Notch1 Positive Progenitor Cells in the Developing Retina. *PLoS One* **10**, e0131054 (2015).
52. Le, T. T., Wroblewski, E., Patel, S., Riesenberg, A. N. & Brown, N. L. Math5 is required for both early retinal neuron differentiation and cell cycle progression. *Dev. Biol.* **295**, 764–778 (2006).
53. Paolini, A. *et al.* Asymmetric inheritance of the apical domain and self-renewal of retinal ganglion cell progenitors depend on Anillin function. *Development* **142**, 832–839 (2015).
54. Diao, Y., Chen, Y., Zhang, P., Cui, L. & Zhang, J. Molecular guidance cues in the development of visual pathway. *Protein Cell* **9**, 909–929 (2018).
55. Gregory-Evans, C. Y., Wallace, V. A. & Gregory-Evans, K. Gene networks: Dissecting pathways in retinal development and disease. *Prog. Retin. Eye Res.* **33**, 40–66 (2013).
56. Fadool, J. & Dowling, J. Zebrafish: A model system for the study of eye genetics. *Prog. Retin. Eye Res.* **27**, 89–110 (2008).
57. Glass, A. S. & Dahm, R. The Zebrafish as a Model Organism for Eye Development. *Ophthalmic Res.* **36**, 4–24 (2004).
58. Aose, M. *et al.* The occhiolino (occ) mutant Zebrafish, a model for development of the optical function in the biological lens. *Dev. Dyn.* (2017). doi:10.1002/dvdy.24511
59. Cavodeassi, F. & Wilson, S. W. Looking to the future of zebrafish as a model to understand the genetic basis of eye disease. *Hum. Genet.* **138**, 993–1000 (2019).
60. Dill, H. & Fischer, U. Gene Knockdown in Zebrafish (Danio rerio) as a Tool to Model Photoreceptor Diseases. in *Methods in Molecular Biology* (2019). doi:10.1007/978-1-4939-8669-9_15
61. Gestri, G., Link, B. A. & Neuhauss, S. C. F. The visual system of zebrafish and its use to model human ocular Diseases. *Dev. Neurobiol.* **72**, 302–327 (2012).
62. Posner, M., McDonald, M. S., Murray, K. L. & Kiss, A. J. Why does the zebrafish cloche mutant develop lens cataract? *PLoS One* **14**, 1–16 (2019).
63. Richardson, R., Tracey-White, D., Webster, A. & Moosajee, M. The zebrafish eye—a paradigm for investigating human ocular genetics Zebrafish as a model organism. *Nat. Publ. Gr.* (2016). doi:10.1038/eye.2016.198
64. Santoriello, C. & Zon, L. I. Hooked ! Modeling human disease in zebrafish. *Sci. Med.* **122**, 2337–2343 (2012).
65. Lin, H. J., Hong, Z. Y., Li, Y. K. & Liau, I. Fluorescent tracer of dopamine enables selective labelling and interrogation of dopaminergic amacrine cells in the retina of living zebrafish.

RSC Adv. (2016). doi:10.1039/c6ra13073a

66. Ma, M. *et al.* Zebrafish Dscaml1 is Essential for Retinal Patterning and Function of Oculomotor Subcircuits. *bioRxiv* (2019). doi:10.1101/658161
67. Mochizuki, T. & Masai, I. The lens equator: A platform for molecular machinery that regulates the switch from cell proliferation to differentiation in the vertebrate lens. *Dev. Growth Differ.* **56**, 387–401 (2014).
68. Vacaru, A. M. *et al.* In vivo cell biology in zebrafish - providing insights into vertebrate development and disease. *J. Cell Sci.* **127**, 485–495 (2014).
69. Kitambi, S. S., McCulloch, K. J., Peterson, R. T. & Malicki, J. J. Small molecule screen for compounds that affect vascular development in the zebrafish retina. *Mech. Dev.* **126**, 464–477 (2009).
70. Stewart, A. M., Braubach, O., Spitsbergen, J., Gerlai, R. & Kalueff, A. V. Zebrafish models for translational neuroscience research: from tank to bedside. *Trends Neurosci.* **37**, 264–278 (2014).
71. Ward, R. *et al.* Pharmacological restoration of visual function in a zebrafish model of von-Hippel Lindau disease. *Dev. Biol.* (2020). doi:10.1016/j.ydbio.2019.02.008
72. Zon, L. I. & Peterson, R. T. In vivo drug discovery in the zebrafish. *Nat. Rev. Drug Discov.* **4**, 35–44 (2005).
73. Kimmel, C. B., Ballard, W. W., Kimmel, S. R., Ullmann, B. & Schilling, T. F. Stages of embryonic development of the zebrafish. *Dev. Dyn.* (1995). doi:10.1002/aja.1002030302
74. McNabb, A., Scott, K., Ochsenstein, E. Von, Seufert, K. & Carl, M. Don't be afraid to set up your fish facility. *Zebrafish* (2012). doi:10.1089/zeb.2012.0768
75. Weidinger, G., Thorpe, C. J., Wuennenberg-Stapleton, K., Ngai, J. & Moon, R. T. The Sp1-related transcription factors sp5 and sp5-like act downstream of Wnt/β-catenin signaling in mesoderm and neuroectoderm patterning. *Curr. Biol.* **15**, 489–500 (2005).
76. Flicek, P. *et al.* Ensembl 2013. *Nucleic Acids Res.* (2013). doi:10.1093/nar/gks1236
77. Johnson, W. E., Li, C. & Rabinovic, A. Adjusting batch effects in microarray expression data using empirical Bayes methods. *Biostatistics* (2007). doi:10.1093/biostatistics/kxj037
78. Ritchie, M. E. *et al.* Limma powers differential expression analyses for RNA-sequencing and microarray studies. *Nucleic Acids Res.* (2015). doi:10.1093/nar/gkv007
79. Durinck, S., Spellman, P. T., Birney, E. & Huber, W. Mapping identifiers for the integration of genomic datasets with the R/ Bioconductor package biomaRt. *Nat. Protoc.* (2009). doi:10.1038/nprot.2009.97
80. Zhou, Y. *et al.* Metascape provides a biologist-oriented resource for the analysis of systems-

level datasets. *Nat. Commun.* (2019). doi:10.1038/s41467-019-09234-6

81. Xie, C. *et al.* KOBAS 2.0: A web server for annotation and identification of enriched pathways and diseases. *Nucleic Acids Res.* (2011). doi:10.1093/nar/gkr483
82. Szklarczyk, D. *et al.* STRING v11: Protein-protein association networks with increased coverage, supporting functional discovery in genome-wide experimental datasets. *Nucleic Acids Res.* (2019). doi:10.1093/nar/gky1131
83. Shannon, P. *et al.* Cytoscape: A software Environment for integrated models of biomolecular interaction networks. *Genome Res.* (2003). doi:10.1101/gr.1239303
84. Langfelder, P. & Horvath, S. WGCNA: An R package for weighted correlation network analysis. *BMC Bioinformatics* (2008). doi:10.1186/1471-2105-9-559
85. Newman, M. E. J. Finding community structure in networks using the eigenvectors of matrices. *Phys. Rev. E - Stat. Nonlinear, Soft Matter Phys.* (2006). doi:10.1103/PhysRevE.74.036104
86. Masai, I., Stemple, D. L., Okamoto, H. & Wilson, S. W. Midline Signals Regulate Retinal Neurogenesis in Zebrafish. *Neuron* **27**, 251–263 (2000).
87. Hu, M., Easter, S. S. J. & Easter, J. Retinal neurogenesis: The formation of the initial central patch of postmitotic cells. *Dev. Biol.* **207**, 309–321 (1999).
88. Gavriouchkina, D. *et al.* Thyrotroph embryonic factor regulates light-induced transcription of repair genes in zebrafish embryonic cells. *PLoS One* (2010). doi:10.1371/journal.pone.0012542
89. Tissir, F. & Goffinet, A. M. Atypical cadherins Celsr1-3 and planar cell polarity in vertebrates. in *Progress in Molecular Biology and Translational Science* (2013). doi:10.1016/B978-0-12-394311-8.00009-1
90. Abouzeid, H. *et al.* RAX and anophthalmia in humans: Evidence of brain anomalies. *Mol. Vis.* (2012).
91. Cantu, J. A., Flowers, G. P. & Topczewski, J. Notum homolog plays a novel role in primary motor innervation. *J. Neurosci.* (2013). doi:10.1523/JNEUROSCI.3694-12.2013
92. Foulquier, F. *et al.* TMEM165 deficiency causes a congenital disorder of glycosylation. *Am. J. Hum. Genet.* **91**, 15–26 (2012).
93. Piekny, A. J. & Maddox, A. S. The myriad roles of Anillin during cytokinesis. *Seminars in Cell and Developmental Biology* (2010). doi:10.1016/j.semcdb.2010.08.002
94. Diacou, R., Zhao, Y., Zheng, D., Cvekl, A. & Liu, W. Six3 and Six6 Are Jointly Required for the Maintenance of Multipotent Retinal Progenitors through Both Positive and Negative Regulation. *Cell Rep.* **25**, 2510-2523.e4 (2018).

95. Loosli, F. *et al.* Loss of eyes in zebrafish caused by mutation of chokh/rx 3. *EMBO Rep.* (2003). doi:10.1038/sj.embor.embor919

96. Nelson, S. M., Park, L. & Stenkamp, D. L. Retinal homeobox 1 is required for retinal neurogenesis and photoreceptor differentiation in embryonic zebrafish. *Dev. Biol.* **328**, 24–39 (2009).

97. Markitantova, Y. & Simirskii, V. *Inherited eye diseases with retinal manifestations through the eyes of homeobox genes*. *International Journal of Molecular Sciences* **21**, (2020).

98. Hehr, C. L., Hocking, J. C. & McFarlane, S. Matrix metalloproteinases are required for retinal ganglion cell axon guidance at select decision points. *Development* (2005). doi:10.1242/dev.01908

99. Janssens, E. *et al.* Matrix Metalloproteinase 14 in the Zebrafish: An Eye on Retinal and Retinotectal Development. *PLoS One* **8**, e52915 (2013).

100. Lemmens, K. *et al.* Matrix metalloproteinases as promising regulators of axonal regrowth in the injured adult zebrafish retinotectal system. *J. Comp. Neurol.* (2016). doi:10.1002/cne.23920

101. Piri, N., Kwong, J. M. K., Gu, L. & Caprioli, J. Heat shock proteins in the retina: Focus on HSP70 and alpha crystallins in ganglion cell survival. *Prog. Retin. Eye Res.* **52**, 22–46 (2016).

102. Cvekl, A. & Mitton, K. P. Epigenetic regulatory mechanisms in vertebrate eye development and disease. *Heredity* (2010). doi:10.1038/hdy.2010.16

103. Scheidecker, S. *et al.* Mutations in TUBGCP4 alter microtubule organization via the γ-tubulin ring complex in autosomal-recessive microcephaly with chorioretinopathy. *Am. J. Hum. Genet.* (2015). doi:10.1016/j.ajhg.2015.02.011

104. Blixt, M. K. E., Konjusha, D., Ring, H. & Hallböök, F. Zinc finger gene nolz1 regulates the formation of retinal progenitor cells and suppresses the Lim3/Lhx3 phenotype of retinal bipolar cells in chicken retina. *Dev. Dyn.* **247**, 630–641 (2018).

105. Paridaen, J. T. M. L. *et al.* The nucleolar GTP-binding proteins Gnl2 and nucleostemin are required for retinal neurogenesis in developing zebrafish. *Dev. Biol.* **355**, 286–301 (2011).

106. Agathocleous, M. & Harris, W. A. From Progenitors to Differentiated Cells in the Vertebrate Retina. *Annu. Rev. Cell Dev. Biol.* **25**, 45–69 (2009).

107. Reinhardt, R. *et al.* Sox2, Tlx, Gli3, and Her9 converge on Rx2 to define retinal stem cells in vivo . *EMBO J.* (2015). doi:10.15252/embj.201490706

108. Furukawa, T., Kozak, C. A. & Cepko, C. L. rax, a novel paired-type homeobox gene, shows expression in the anterior neural fold and developing retina. *Proc. Natl. Acad. Sci. U. S. A.*

(1997). doi:10.1073/pnas.94.7.3088

109. Loosli, F. *et al.* Medaka eyeless is the key factor linking retinal determination and eye growth. *Development* (2001).
110. Mathers, P. H., Grinberg, A., Mahon, K. A. & Jamrich, M. The Rx homeobox gene is essential for vertebrate eye development. *Nature* (1997). doi:10.1038/42475
111. Chassaing, N. *et al.* Molecular findings and clinical data in a cohort of 150 patients with anophthalmia/microphthalmia. *Clin. Genet.* (2014). doi:10.1111/cge.12275
112. Lequeux, L. *et al.* Confirmation of RAX gene involvement in human anophthalmia. *Clin. Genet.* **74**, 392–395 (2008).
113. Voronina, V. A. *et al.* Mutations in the human RAX homeobox gene in a patient with anophthalmia and sclerocornea. *Hum. Mol. Genet.* (2004). doi:10.1093/hmg/ddh025
114. Aldahmesh, M. A., Khan, A. O., Hijazi, H. & Alkuraya, F. S. Homozygous truncation of SIX6 causes complex microphthalmia in humans. *Clinical Genetics* (2013). doi:10.1111/cge.12046
115. Teotia, P. *et al.* Modeling Glaucoma: Retinal Ganglion Cells Generated from Induced Pluripotent Stem Cells of Patients with SIX6 Risk Allele Show Developmental Abnormalities. *Stem Cells* (2017). doi:10.1002/stem.2675
116. Chen, Y. *et al.* Genetic variants associated with different risks for high tension glaucoma and normal tension glaucoma in a Chinese population. *Investig. Ophthalmol. Vis. Sci.* (2015). doi:10.1167/iovs.14-16269
117. Khawaja, A. P. *et al.* Genome-wide analyses identify 68 new loci associated with intraocular pressure and improve risk prediction for primary open-angle glaucoma. *Nat. Genet.* (2018). doi:10.1038/s41588-018-0126-8
118. Mabuchi, F. *et al.* Involvement of genetic variants associated with primary open-angle glaucoma in pathogenic mechanisms and family history of glaucoma. *Am. J. Ophthalmol.* (2015). doi:10.1016/j.ajo.2014.11.023
119. Yariz, K. O. *et al.* A homozygous SIX6 mutation is associated with optic disc anomalies and macular atrophy and reduces retinal ganglion cell differentiation. *Clin. Genet.* **87**, 192–195 (2015).
120. Khan, A. O. Genetics of primary glaucoma. *Current Opinion in Ophthalmology* (2011). doi:10.1097/ICU.0b013e32834922d2
121. Reis, L. M. & Semina, E. V. Conserved genetic pathways associated with microphthalmia, anophthalmia, and coloboma. *Birth Defects Research Part C - Embryo Today: Reviews* (2015). doi:10.1002/bdrc.21097

122. Goodwin, L. R. & Picketts, D. J. The role of ISWI chromatin remodeling complexes in brain development and neurodevelopmental disorders. *Molecular and Cellular Neuroscience* (2018). doi:10.1016/j.mcn.2017.10.008

123. Das, A. V. *et al.* SWI/SNF chromatin remodeling ATPase Brm regulates the differentiation of early retinal stem cells/progenitors by influencing Brn3b expression and Notch signaling. *J. Biol. Chem.* (2007). doi:10.1074/jbc.M706742200

124. He, S. *et al.* Chromatin remodeling enzyme Snf2h regulates embryonic lens differentiation and denucleation. *Dev.* (2016). doi:10.1242/dev.135285

125. Gross, J. M. *et al.* Identification of Zebrafish insertional mutants with defects in visual system development and function. *Genetics* (2005). doi:10.1534/genetics.104.039727

126. Martins, D., Moreira, J., Gonçalves, N. P. & Saraiva, M. J. MMP-14 overexpression correlates with the neurodegenerative process in familial amyloidotic polyneuropathy. *DMM Dis. Model. Mech.* (2017). doi:10.1242/dmm.028571

127. Nagashima, M., Fujikawa, C., Mawatari, K., Mori, Y. & Kato, S. HSP70, the earliest-induced gene in the zebrafish retina during optic nerve regeneration: Its role in cell survival. *Neurochem. Int.* **58**, 888–895 (2011).

128. Fujikawa, C., Nagashima, M., Mawatari, K. & Kato, S. HSP70 gene expression in the zebrafish retina after optic nerve injury: A comparative study under heat shock stresses. in *Advances in Experimental Medicine and Biology* **723**, 663–668 (2012).

129. Sinha, D. *et al.* βA3/A1-crystallin in astroglial cells regulates retinal vascular remodeling during development. *Mol. Cell. Neurosci.* **37**, 85–95 (2008).

130. Drankowska, J. *et al.* MMP targeting in the battle for vision: Recent developments and future prospects in the treatment of diabetic retinopathy. *Life Sciences* (2019). doi:10.1016/j.lfs.2019.05.038

131. Kubo, F., Takeichi, M. & Nakagawa, S. Wnt2b inhibits differentiation of retinal progenitor cells in the absence of Notch activity by downregulating the expression of proneural genes. *Development* (2005). doi:10.1242/dev.01856

132. Masai, I., Yamaguchi, M., Tonou-Fujimori, N., Komori, A. & Okamoto, H. The hedgehog-PKA pathway regulates two distinct steps of the differentiation of retinal ganglion cells: The cell-cycle exit of retinoblasts and their neuronal maturation. *Development* (2005). doi:10.1242/dev.01714

133. Souren, M., Martinez-Morales, J. R., Makri, P., Wittbrodt, B. & Wittbrodt, J. A global survey identifies novel upstream components of the Ath5 neurogenic network. *Genome Biol.* (2009). doi:10.1186/gb-2009-10-9-r92

134. Shima, Y. *et al.* Opposing roles in neurite growth control by two seven-pass transmembrane cadherins. *Nat. Neurosci.* (2007). doi:10.1038/nn1933

135. Hackam, A. S. The Wnt signaling pathway in retinal degenerations. *IUBMB Life* **57**, 381–388 (2005).

136. Poggi, L., Casarosa, S. & Carl, M. An Eye on the Wnt Inhibitory Factor Wif1. *Front. Cell Dev. Biol.* **6**, (2018).

137. Shastry, B. S. Persistent hyperplastic primary vitreous: congenital malformation of the eye. *Clin. Experiment. Ophthalmol.* **37**, 884–890 (2009).

138. Bats, M. L. *et al.* Therapies targeting Frizzled-7/β-catenin pathway prevent the development of pathological angiogenesis in an ischemic retinopathy model. *FASEB J.* **34**, 1288–1303 (2020).

139. Fujimura, N. WNT/β-catenin signaling in vertebrate eye development. *Frontiers in Cell and Developmental Biology* (2016). doi:10.3389/fcell.2016.00138

140. Mills, E. A. & Goldman, D. The Regulation of Notch Signaling in Retinal Development and Regeneration. *Current Pathobiology Reports* (2017). doi:10.1007/s40139-017-0153-7

141. Nelson, B. R., Gumuscu, B., Hartman, B. H. & Reh, T. A. Notch activity is downregulated just prior to retinal ganglion cell differentiation. *Dev. Neurosci.* (2006). doi:10.1159/000090759

142. Ohnuma, S. I., Hopper, S., Wang, K. C., Philpott, A. & Harris, W. A. Co-ordinating retinal histogenesis: Early cell cycle exit enhances early cell fate determination in the Xenopus retina. *Development* (2002).

143. Del Bene, F., Wehman, A. M., Link, B. A. & Baier, H. Regulation of Neurogenesis by Interkinetic Nuclear Migration through an Apical-Basal Notch Gradient. *Cell* (2008). doi:10.1016/j.cell.2008.07.017

144. Cepero Malo, M. *et al.* The Zebrafish Anillin-eGFP Reporter Marks Late Dividing Retinal Precursors and Stem Cells Entering Neuronal Lineages. *PLoS One* **12**, e0170356 (2017).

145. Zhang, L. & Maddox, A. S. Anillin. *Current Biology* (2010). doi:10.1016/j.cub.2009.12.017

146. Dai, X., Chen, X., Hakizimana, O. & Mei, Y. Genetic interactions between ANLN and KDR are prognostic for breast cancer survival. *Oncol. Rep.* (2019). doi:10.3892/or.2019.7332

147. Gbadegesin, R. A. *et al.* Mutations in the gene that encodes the F-Actin binding protein anillin cause FSGS. *J. Am. Soc. Nephrol.* **25**, 1991–2002 (2014).

148. Hall, G. *et al.* The Human FSGS-Causing ANLN R431C Mutation Induces Dysregulated PI3K/AKT/mTOR/Rac1 Signaling in Podocytes. *J. Am. Soc. Nephrol.* **29**, 2110–2122 (2018).

149. Lian, Y. F. *et al.* Anillin is required for tumor growth and regulated by miR-15a/miR- 16-1 in HBV-related hepatocellular carcinoma. *Aging (Albany. NY).* **10**, 1884–1901 (2018).

150. Tian, D. *et al.* Anillin regulates neuronal migration and neurite growth by linking RhoG to the actin cytoskeleton. *Curr. Biol.* (2015). doi:10.1016/j.cub.2015.02.072

151. Rehain, K. & Maddox, A. S. Neuron migration: Anillin protects leading edge actin. *Current Biology* **25**, R423–R425 (2015).

152. Erwig, M. S. *et al.* Anillin facilitates septin assembly to prevent pathological outfoldings of central nervous system myelin. *Elife* (2019). doi:10.7554/eLife.43888

153. Patzig, J. *et al.* Septin/anillin filaments scaffold central nervous system myelin to accelerate nerve conduction. *Elife* (2016). doi:10.7554/eLife.17119.001

154. Pandi, N. S. *et al.* In silico analysis of expression pattern of a Wnt/β-catenin responsive gene ANLN in gastric cancer. *Gene* **545**, 23–29 (2014).

155. Reyes, C. C. *et al.* Anillin regulates cell-cell junction integrity by organizing junctional accumulation of Rho-GTP and actomyosin. *Curr. Biol.* (2014). doi:10.1016/j.cub.2014.04.021

156. Wang, D., Naydenov, N. G., Dozmorov, M. G., Koblinski, J. E. & Ivanov, A. I. Anillin regulates breast cancer cell migration , growth , and metastasis by non- canonical mechanisms involving control of cell stemness and differentiation. *Breast cancer Res.* 1–19 (2020).

157. Fagotto, F. Looking beyond the Wnt pathway for the deep nature of β-catenin. *EMBO Reports* (2013). doi:10.1038/embor.2013.45

158. Tian, X. *et al.* E-Cadherin/β-catenin complex and the epithelial barrier. *J. Biomed. Biotechnol.* **2011**, (2011).

159. Nusse, R. & Clevers, H. Wnt/β-Catenin Signaling, Disease, and Emerging Therapeutic Modalities. *Cell* (2017). doi:10.1016/j.cell.2017.05.016

160. Yao, K. *et al.* Wnt Regulates Proliferation and Neurogenic Potential of Müller Glial Cells via a Lin28/let-7 miRNA-Dependent Pathway in Adult Mammalian Retinas. *Cell Rep.* **17**, 165–178 (2016).

161. Meyers, J. R. *et al.* β-catenin/Wnt signaling controls progenitor fate in the developing and regenerating zebrafish retina. *Neural Dev.* (2012). doi:10.1186/1749-8104-7-30

162. Alizadeh, E., Mammadzada, P. & André, H. The Different Facades of Retinal and Choroidal Endothelial Cells in Response to Hypoxia. *Int. J. Mol. Sci.* **19**, 3846 (2018).

163. Smith, J. R., David, L. L., Appukuttan, B. & Wilmarth, P. A. *Angiogenic and Immunologic Proteins Identified by Deep Proteomic Profiling of Human Retinal and Choroidal Vascular*

Endothelial Cells: Potential Targets for New Biologic Drugs. *American Journal of Ophthalmology* **193**, (Elsevier Inc., 2018).

164. Weger, B. D. *et al.* The light responsive transcriptome of the Zebrafish: Function and regulation. *PLoS One* (2011). doi:10.1371/journal.pone.0017080
165. Baba, K. *et al.* Removal of clock gene Bmal1 from the retina affects retinal development and accelerates cone photoreceptor degeneration during aging. *Proc. Natl. Acad. Sci. U. S. A.* (2018). doi:10.1073/pnas.1808137115
166. Stone, R. A. *et al.* Altered ocular parameters from circadian clock gene disruptions. *PLoS One* (2019). doi:10.1371/journal.pone.0217111
167. Sawant, O. B. *et al.* The circadian clock gene Bmal1 is required to control the timing of retinal neurogenesis and lamination of Müller glia in the mouse retina. *FASEB J.* (2019). doi:10.1096/fj.201801832RR
168. Laranjeiro, R. & Whitmore, D. Transcription factors involved in retinogenesis are co-opted by the circadian clock following photoreceptor differentiation. *Dev.* (2014). doi:10.1242/dev.104380
169. Felder-Schmittbuhl, M.-P., Calligaro, H. & Dkhissi-Benyahya, O. The retinal clock in mammals: role in health and disease. *ChronoPhysiology Ther.* (2017). doi:10.2147/cpt.s115251

FIGURE LEGENDS

Figure 1: Scheme of the experimental design for the comparative marray analysis. *A)* Confocal images showing examples of wild type and *lak-/-* (*lakritz*); *tg(atoh7:gap43-RFP)* embryos at 96 hpf. The RFP-positive optic chiasm and RGCs are absent in the retina of a *lakritz* embryo. *B)* Pairs of eyes were dissected from single embryos at 28-30 hpf embryos. Genotyping on the gDNA extracted from each corresponding cell body was performed to identify *lakritz* and wt embryos (see materials and methods section). The RNA extracted from each pair of eyes corresponding to either a *lakritz* or wt embryo was amplified and used for the microarray analysis and qPCR expression analysis.

Figure 2: Volcano and heatmap of differentially expressed genes in lakritz vs wild-type eyes.

A) Volcano plot highlighting Atoh7 and its direct targets (in red) among all differentially expressed probes (in green) with adjusted p-value < 0.05. *B*) Heatmap was constructed by calculating row Z-score
using normalised log2 intensities of 144 of the 173 differentially expressed probes with corresponding gene annotation, using complete hierarchical clustering in R.

Figure 3: Functional enrichment analysis. *A)* Statistically significantly overrepresented GO Biological Process categories (Metascape). *B)* Significantly differentially expressed genes belonging to the "neural retina development" category **(see also Supplementary Table 2)**.

Figure 4: Interaction network downstream of Atoh7. Known interactions between downstream targets of Atoh7 from the STRING database and visualised with Cytoscape (genes without known interactions are not represented). Node colours represent the log2 fold-change of the gene expression in *lakritz* versus wild type eyes. Node borders are coloured by gene ontology annotation: "neural retina development" (green), "cell cycle process" (yellow), "Wnt signalling pathway" (pink) and "chromatin remodelling" (orange).

Figure 5: Detailed topology of Module 13. Each node represents a gene while a connection represents a co-expression between two genes (only the first 200 edges in order of co-expression weight were retained for visualization purposes). Submodules are shown with decreasing degree of connectivity from left to right. Highlighted edges represent the connection between retina layer formation and wnt - related genes.

Supplementary Figure 1: Batch effect correction.
MDS plots before *A)* and after *B)* batch effect correction using Combat (plotMDS in R).

Supplementary Figure 2: co-expression modules significantly affected by the *lakritz* mutation

Supplementary Figure 3: Functional network analysis on M13: (https://string-db.org/cgi/network.pl?taskId=hNkdhEXQnBhR)

Supplementary Figure 4. Dysregulation of Ctnnb1 localization by *anilin* knock-down and *anillin* expression dynamics. *A)* Ctnnb1 staining in control (ctrlMO, n=3 embryos) versus anilin knock-down (anlnMO, n=3 embryos) in morpholino injected embryos at 30hpf. Arrows show apical

location, arrowheads show apical-to-basal location. *B)* Graph showing the normalized Ctnnb1 intensity signal along the basal-to-apical membrane of the apical-most cells in control (n=3 embryos) versus anlnMO (n=2 embryos) injected embryos. The colored line shows the averaged intensity of all lines for the ctrlMO and anlnMO. Boxplot showing the number of peaks of Ctnnb1 signal intensity along the apical surface in ctrlMO (n=3 embryos) versus anlnMO (n=2 embryos) injected embryos. $P<10^{-4}$. Center lines show the medians; crosses show the means; box limits indicate the 25th and 75th percentiles as determined by R software; whiskers extend 1.5 times the interquartile range from the 25th and 75th percentiles, data points are represented as circles. Student's t-test. *C) Anillin* mRNA levels show dynamic variations during subsequent developmental stages. qPCR was performed on eyes from *lakritz* or wild type embryos at 25, 35, 48, 72 (left) and 96 hpf (right) to assess the trend of *anillin* and *atoh7* expression. The relative gene expression (*lakritz* vs wild type) was calculated using the CT method for each stage. Histogram values are expressed as mean ± s.e.m. ($p < 0.05$) and the mRNA levels of both *gapdh* and *ube2a* were used as internal controls. The statistical analysis is described in the methods section.

Supplementary Table 1: Complete microarray dataset after normalisation and batch correction.

Supplementary Table 2: Gene Ontology enrichment output from Metascape (Biological Process)

Supplementary Table 3: Kobas-based analysis underscores "neural retina development" (GO:0003407) as the most enriched category.

Supplementary Table 4: Weighted gene co-expression network analysis shows Module 3 and 13 with highly interconnected genes.

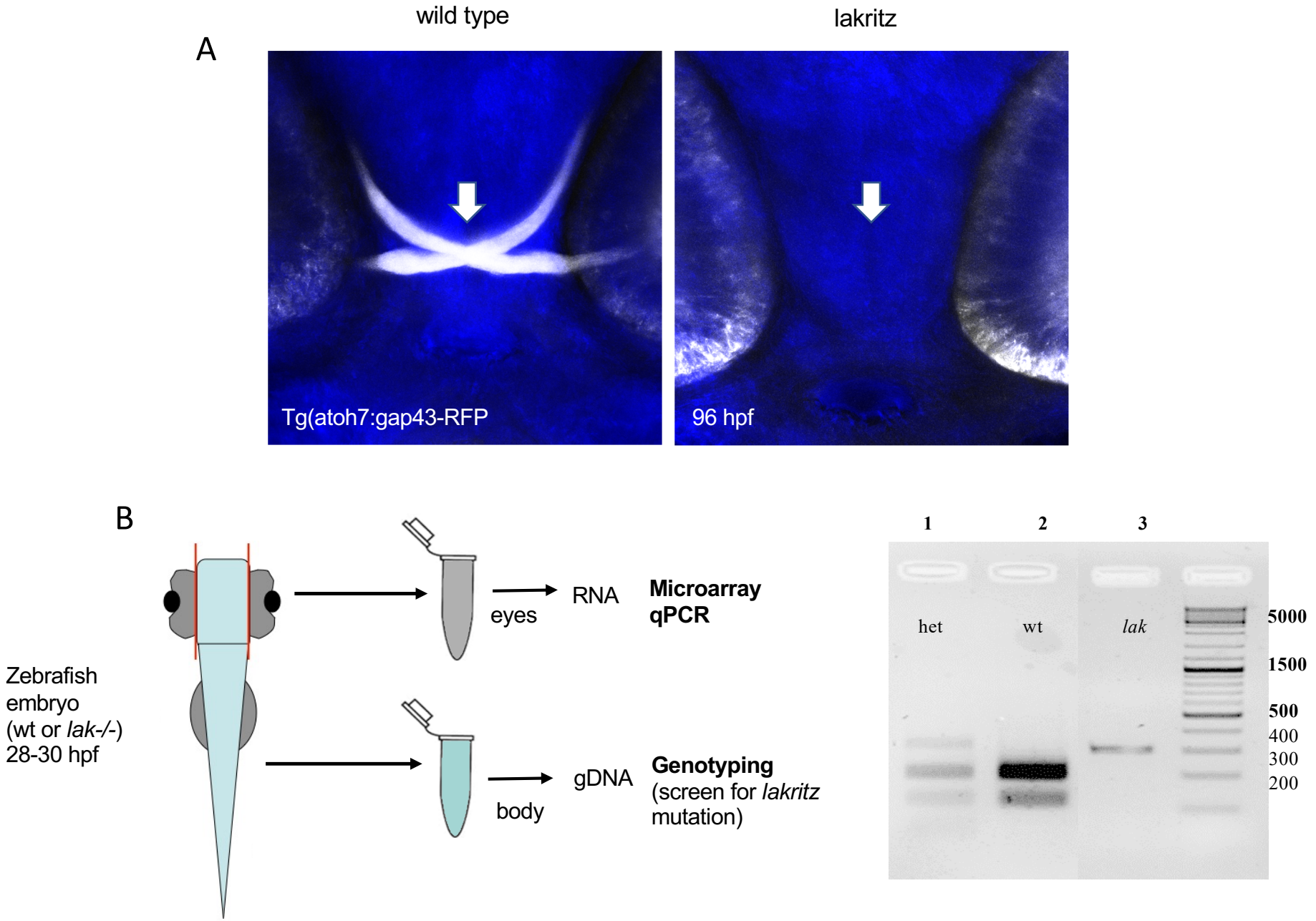
A
wild type
lakritz
Tg(atoh7:gap43-RFP
96 hpf
B
Zebrafish
embryo
(wt or lak-/-)
28-30 hpf
eyes
RNA
Microarray
qPCR
body
gDNA
Genotyping
(screen for lakritz
mutation)
1
2
3
het
wt
lak
5000
1500
500
400
300
200

FIGURE 1

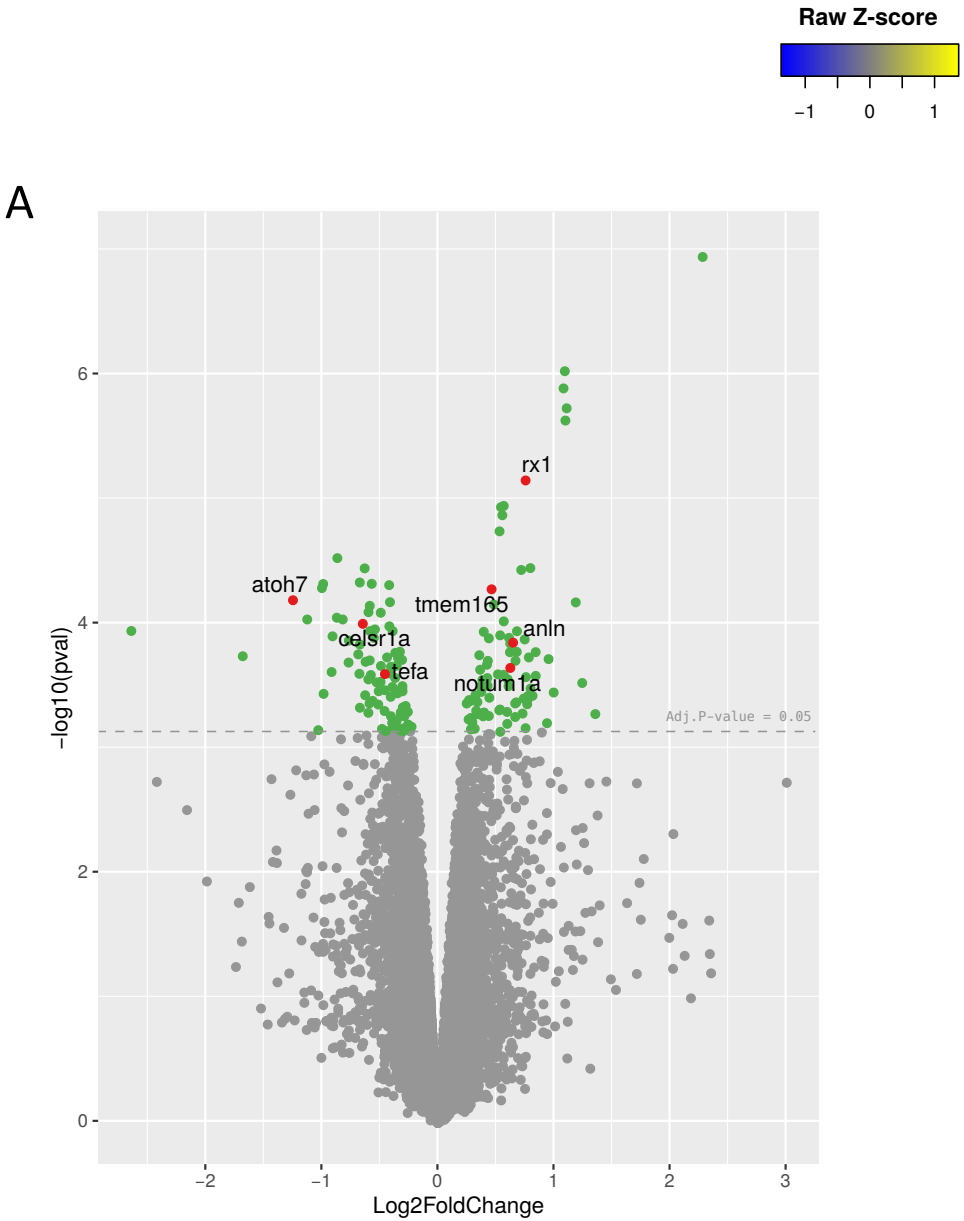
A
Raw Z-score
−1
0
1
6
4
2
0
−log10(pval)
rx1
atoh7
tmem165
anln
celsr1a
tefa
notum1a
Adj.P-value = 0.05
−2
−1
0
1
2
3
Log2FoldChange

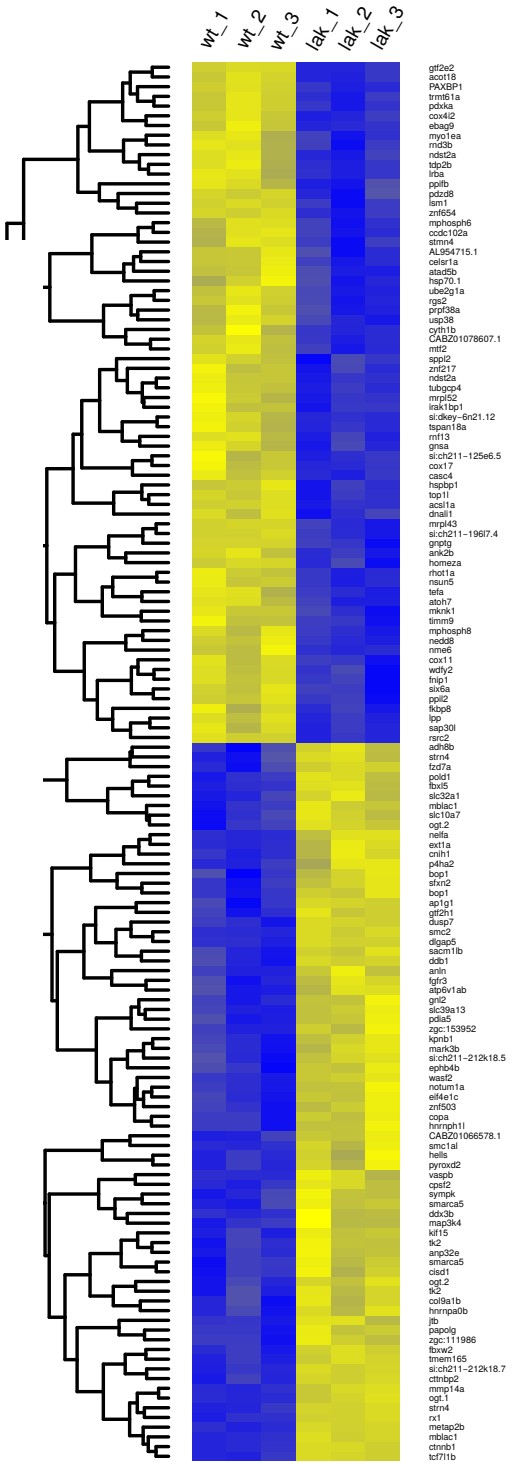
wt_1
wt_2
wt_3
lak_1
lak_2
lak_3
B

FIGURE 2

A

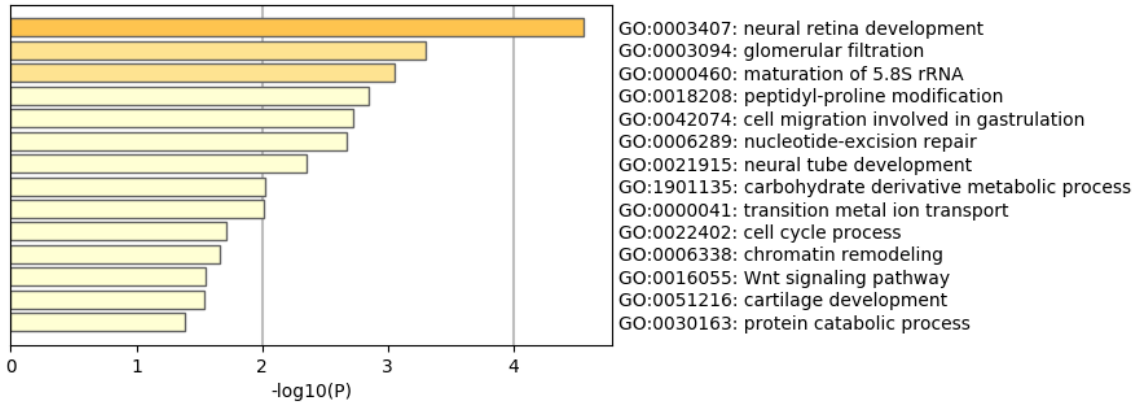

B

GO:0003407 neural retina development					
Input ID	Gene Symbol	H Gene ID	Synonyms	Orphanet	OMIM
ENSDARG00000005374	tubgcp4	**TUBGCP4**	76P|GCP-4|GCP4|Grip76|MCCRP3	[2518] Autosomal recessive chorioretinopathy - microcephaly	OMIM:609610
ENSDARG00000098080	gnl2	**GNL2**	HUMAUANTIG|NGP1|Ngp-1|Nog2|Nug2		OMIM:609365
ENSDARG00000052348	smarca5	**SMARCA5**	ISWI|SNF2H|WCRF135|hISWI|hSNF2H	[370334] Extraskeletal Ewing sarcoma	OMIM:603375
ENSDARG00000002235	mmp14a	**MMP14**	MMP-14|MMP-X1|MT-MMP|MT-MMP 1|MT1-MMP|MT1MMP|MTMMP1|WNCHRS	[85196] Nodulosis-arthropathy-osteolysis syndrome;[3460] TORG-WINCHESTER SYNDROME	OMIM:600754
ENSDARG00000018492	znf503	**ZNF503**	NOLZ-1|NOLZ1|Nlz2		OMIM:613902
ENSDARG00000025187	six6a	**SIX6**	MCOPCT2|ODRMD|OPTX2|Six9	[264200] 14q22q23 microdeletion syndrome;[435930] Colobomatous optic disc-macular atrophy-chorioretinopathy syndrome;[2542] Isolated anophthalmia - microphthalmia	OMIM:606326
ENSDARG00000029688	hsp70.1	**HSPA1L**	HSP70-1L|HSP70-HOM|HSP70T|hum70t		OMIM:140559
ENSDARG00000069552	atoh7	**ATOH7**	Math5|NCRNA|PHPVAR|RNANC|bHLHa13	[289499] Congenital cataract microcornea with corneal opacity;[91495] Persistent hyperplastic primary vitreous	OMIM:609875
ENSDARG00000071684	rx1	**RAX**	RX |MCOP3	[2542] Isolated microphthalmia-anophthalmia-coloboma	OMIM:601881

FIGURE 3

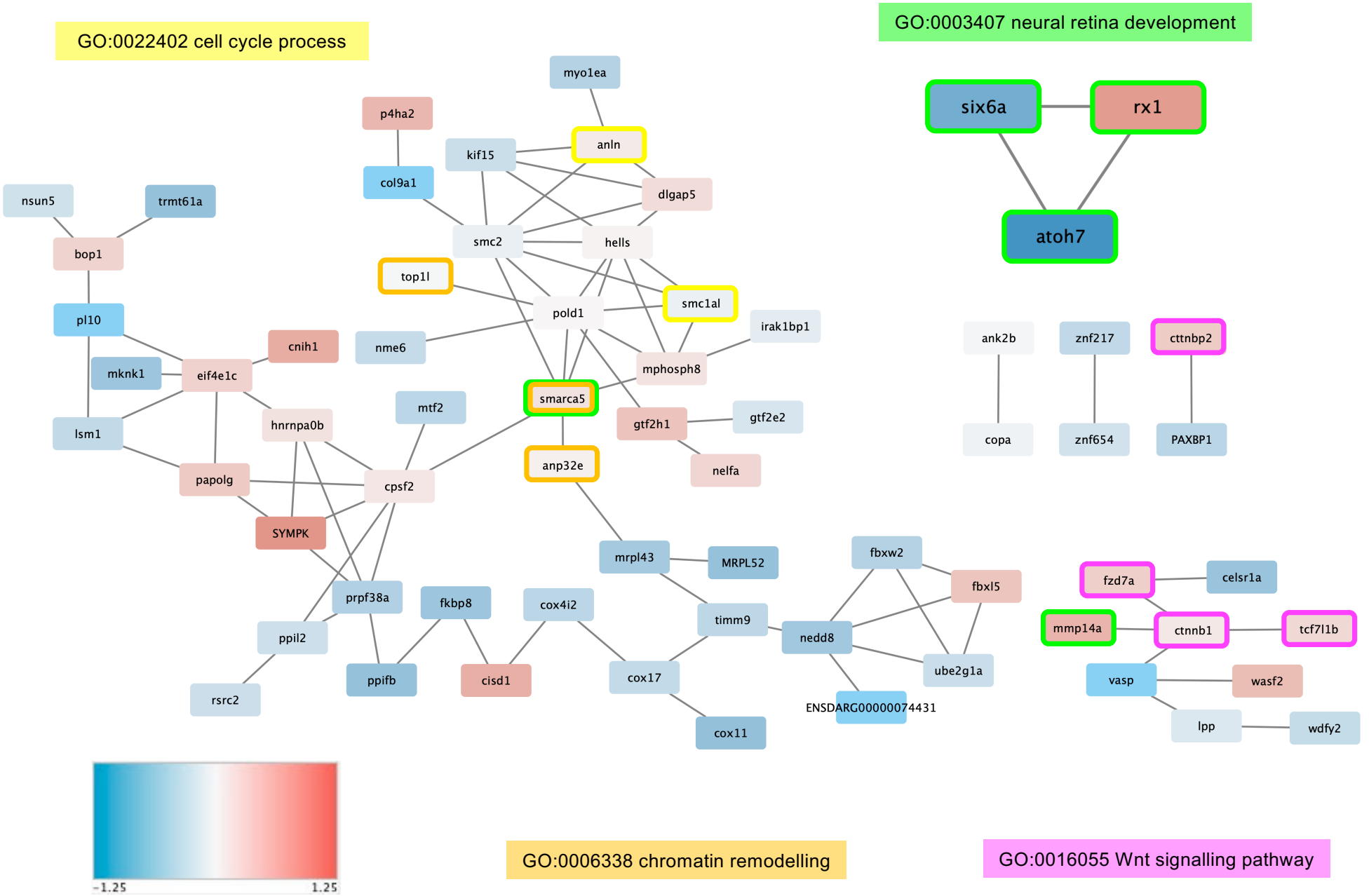
GO:0022402 cell cycle process
GO:0003407 neural retina development
six6a
rx1
atoh7
myo1ea
p4ha2
anln
kif15
col9a1
dlgap5
nsun5
trmt61a
smc2
hells
bop1
top1l
smc1al
pold1
irak1bp1
pl10
nme6
cnih1
mphosph8
mknk1
eif4e1c
smarca5
mtf2
hnrnpa0b
gtf2h1
gtf2e2
lsm1
anp32e
nelfa
papolg
cpsf2
SYMPK
mrpl43
MRPL52
prpf38a
fkbp8
cox4i2
timm9
ppil2
nedd8
ppifb
cisd1
cox17
ube2g1a
rsrc2
cox11
ENSDARG00000074431
fbxw2
fbxl5
ank2b
znf217
cttnbp2
copa
znf654
PAXBP1
fzd7a
celsr1a
mmp14a
ctnnb1
tcf7l1b
vasp
wasf2
lpp
wdfy2
-1.25
1.25
GO:0006338 chromatin remodelling
GO:0016055 Wnt signalling pathway

FIGURE 4

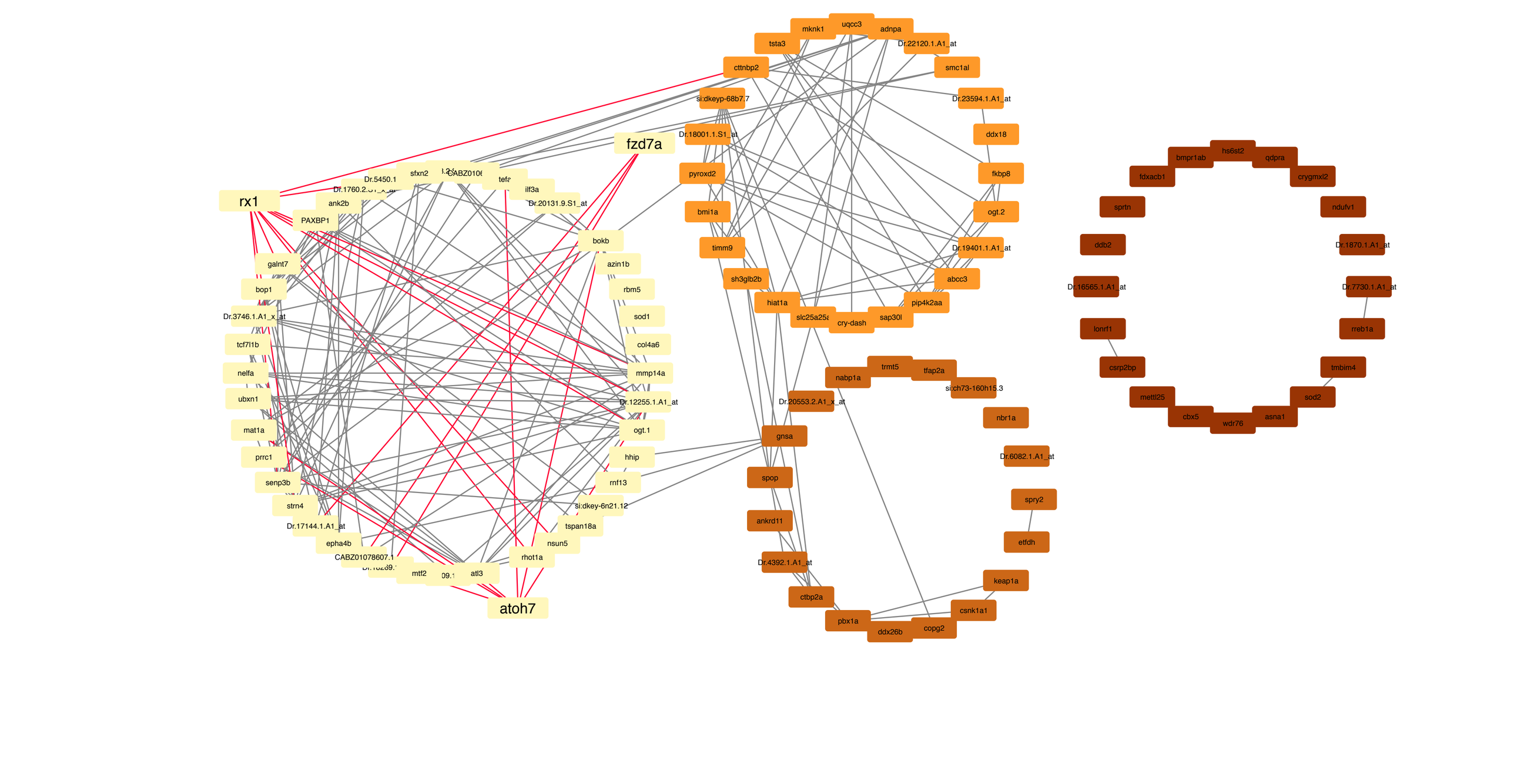
rx1
fzd7a
atoh7
sfxn2
Dr.5450.1
ilf3a
ank2b
Dr.20131.9.S1_at
PAXBP1
bokb
galnt7
azin1b
bop1
rbm5
Dr.3746.1.A1_x_at
sod1
tcf7l1b
col4a6
nelfa
mmp14a
ubxn1
Dr.12255.1.A1_at
mat1a
ogt.1
prrc1
hhip
senp3b
rnf13
strn4
si:dkey-6n21.12
Dr.17144.1.A1_at
tspan18a
epha4b
nsun5
rhot1a
mtf2
atl3
mknk1
uqcc3
adnpa
tsta3
Dr.22120.1.A1_at
cttnbp2
smc1al
si:dkeyp-68b7.7
Dr.23594.1.A1_at
Dr.18001.1.S1_at
ddx18
pyroxd2
fkbp8
bmi1a
ogt.2
timm9
Dr.19401.1.A1_at
sh3glb2b
abcc3
hiat1a
pip4k2aa
cry-dash
sap30l
nabp1a
trmt5
tfap2a
si:ch73-160h15.3
Dr.20553.2.A1_x_at
nbr1a
gnsa
Dr.6082.1.A1_at
spop
spry2
ankrd11
etfdh
Dr.4392.1.A1_at
keap1a
ctbp2a
csnk1a1
pbx1a
ddx26b
copg2
hs6st2
bmpr1ab
qdpra
fdxacb1
crygmxl2
sprtn
ndufv1
ddb2
Dr.1870.1.A1_at
Dr.16565.1.A1_at
Dr.7730.1.A1_at
lonrf1
rreb1a
csrp2bp
tmbim4
mettl25
sod2
cbx5
asna1
wdr76

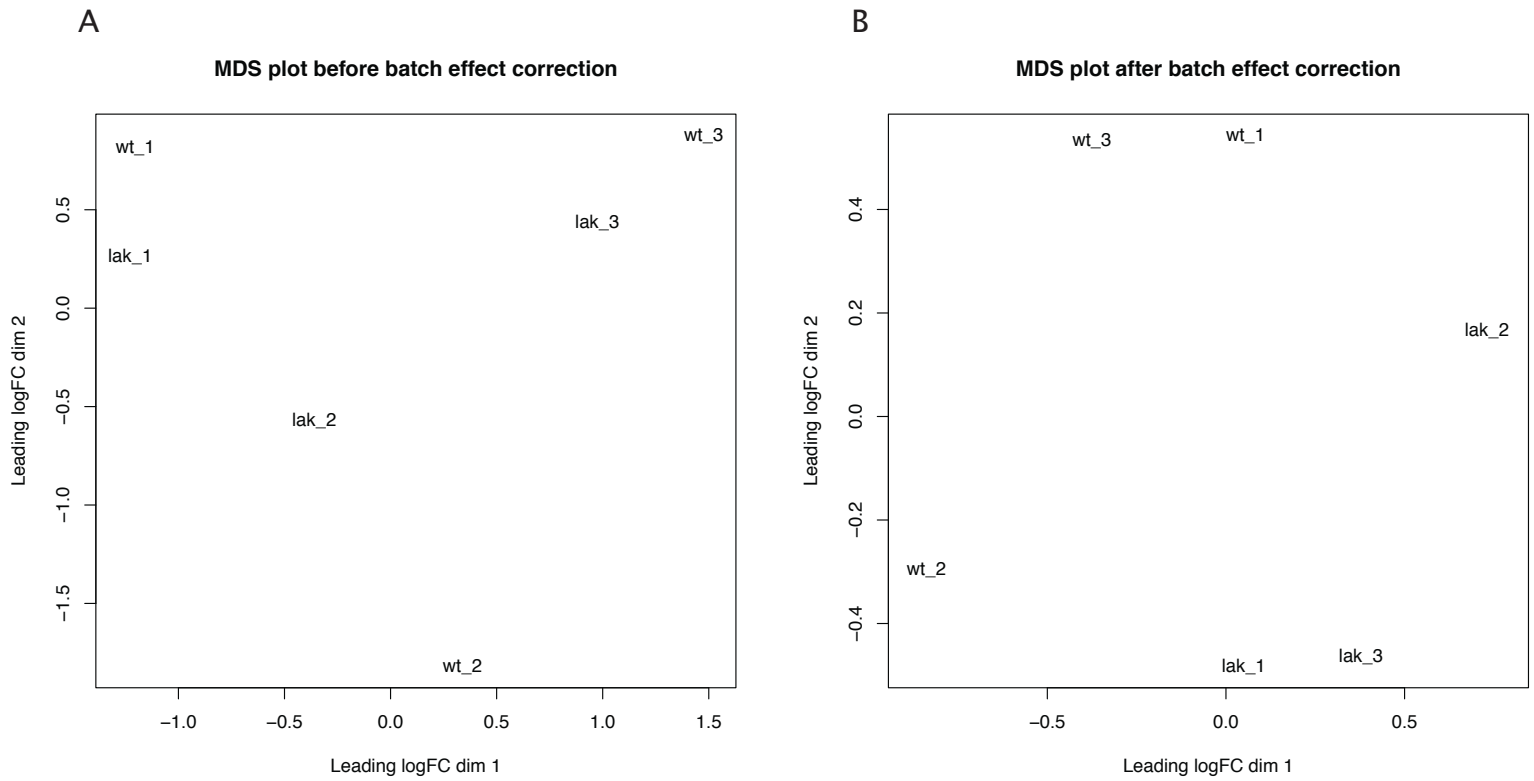

Supplementary Figure 1

Module Correlation with Status and Library Batch

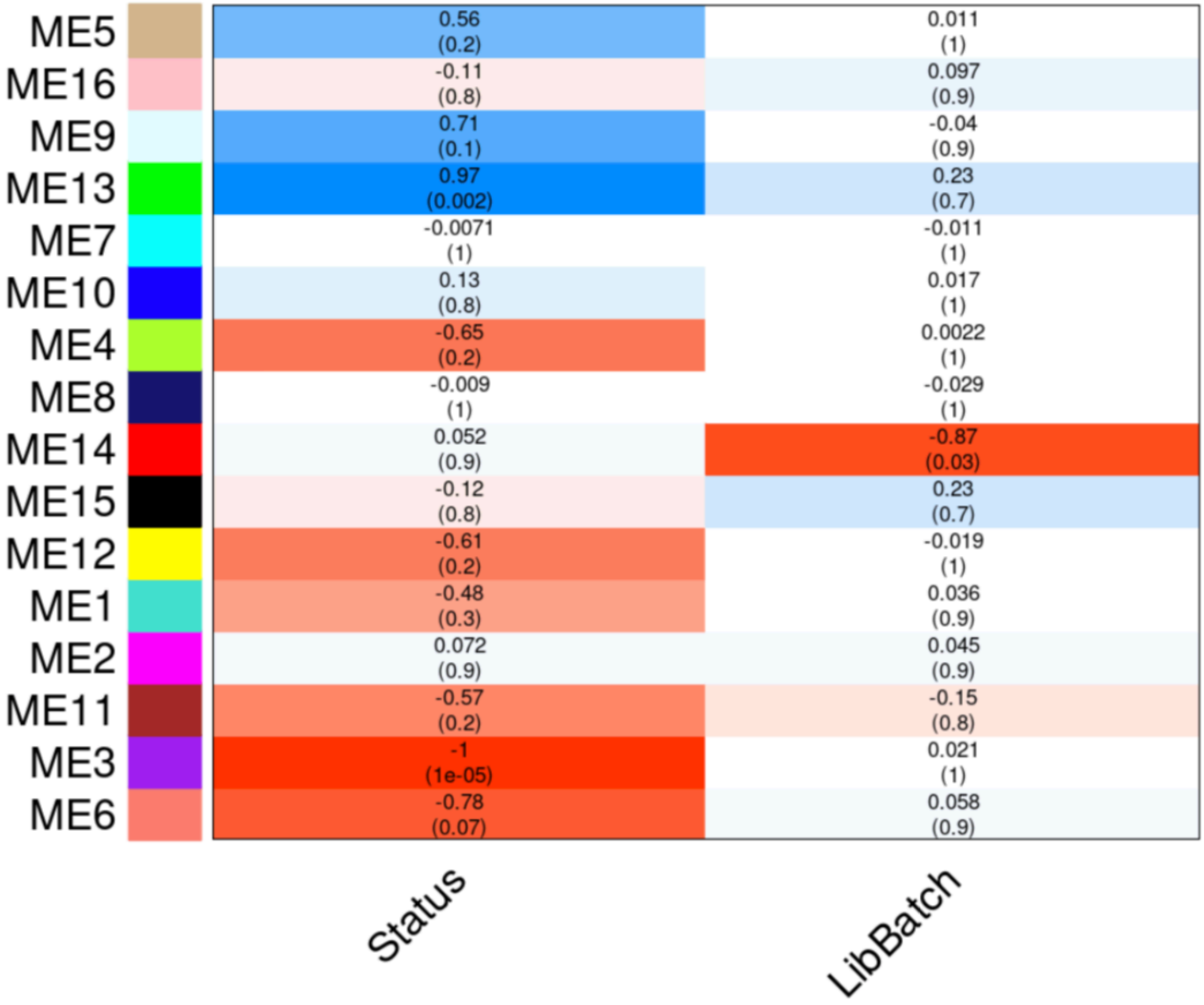

Supplementary Figure 2

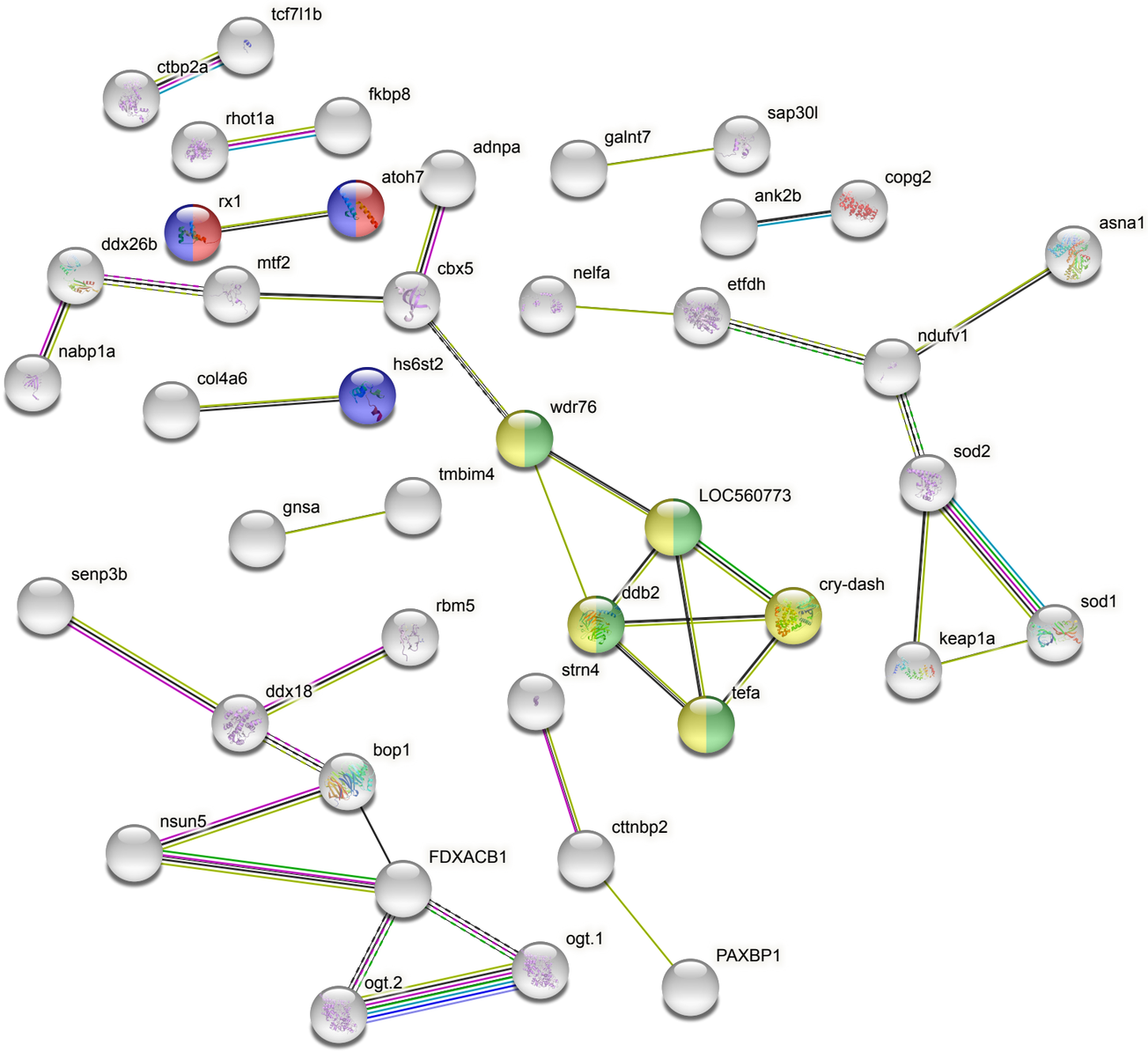

Network Stats

number of nodes:	85	expected number of edges:	22
number of edges:	38	PPI enrichment p-value:	0.000941
average node degree:	0.894	*your network has significantly more interactions than expected (what does that mean?)*	
avg. local clustering coefficient:	0.373		

Functional enrichments in your network

Biological Process (GO)

GO-term	*description*	*count in gene set*	*false discovery rate*
GO:0090304	nucleic acid metabolic process	10 of 689	0.0133
GO:0044237	cellular metabolic process	14 of 1406	0.0133
GO:0033554	cellular response to stress	5 of 145	0.0133
GO:0009987	cellular process	19 of 2089	0.0133
GO:0007006	mitochondrial membrane organization	3 of 15	0.0133
GO:0007005	mitochondrion organization	4 of 68	0.0133
GO:0006839	mitochondrial transport	3 of 37	0.0133
GO:0006807	nitrogen compound metabolic process	13 of 1299	0.0133
GO:0006139	nucleobase-containing compound metabolic process	11 of 771	0.0133
GO:0006974	cellular response to DNA damage stimulus	4 of 100	0.0134
GO:0044260	cellular macromolecule metabolic process	11 of 1006	0.0138
GO:0044238	primary metabolic process	13 of 1373	0.0138
GO:0043170	macromolecule metabolic process	12 of 1174	0.0138
GO:0017004	cytochrome complex assembly	2 of 9	0.0153
GO:0071704	organic substance metabolic process	13 of 1423	0.0168
GO:0010842	retina layer formation	2 of 10	0.0168
GO:0007007	inner mitochondrial membrane organization	2 of 10	0.0168
GO:0097190	apoptotic signaling pathway	2 of 14	0.0273
GO:0033108	mitochondrial respiratory chain complex assembly	2 of 15	0.0284
GO:0065007	biological regulation	12 of 1366	0.0292
GO:0048592	eye morphogenesis	3 of 66	0.0292
GO:0051716	cellular response to stimulus	7 of 522	0.0296
GO:0050896	response to stimulus	8 of 683	0.0306
GO:0006281	DNA repair	3 of 72	0.0311
GO:0071840	cellular component organization or biogenesis	8 of 726	0.0407
GO:0050789	regulation of biological process	11 of 1272	0.0419
GO:0048646	anatomical structure formation involved in morphogenesis	4 of 183	0.0485
GO:0009790	embryo development	5 of 303	0.0485

(less ...)

Molecular Function (GO)

GO-term	*description*	*count in gene set*	*false discovery rate*
GO:0005488	binding	18 of 1569	0.00029
GO:0003677	DNA binding	7 of 372	0.0139
GO:0003684	damaged DNA binding	2 of 7	0.0153
GO:0043167	ion binding	9 of 832	0.0474

Cellular Component (GO)

GO-term	*description*	*count in gene set*	*false discovery rate*
GO:0043231	intracellular membrane-bounded organelle	21 of 1613	3.43e-06
GO:0005739	mitochondrion	7 of 257	0.00027
GO:0044429	mitochondrial part	6 of 179	0.00031
GO:0031966	mitochondrial membrane	5 of 134	0.00082
GO:0044446	intracellular organelle part	12 of 1024	0.00098

GO:0005634	nucleus	12 of 1043	0.0010
GO:0044455	mitochondrial membrane part	3 of 34	0.0014
GO:0032991	protein-containing complex	9 of 631	0.0014
GO:0044444	cytoplasmic part	10 of 1002	0.0077
GO:0032592	integral component of mitochondrial membrane	2 of 16	0.0077
GO:0070013	intracellular organelle lumen	5 of 304	0.0140
GO:0005743	mitochondrial inner membrane	3 of 87	0.0140
GO:0005737	cytoplasm	12 of 1534	0.0146
GO:0044428	nuclear part	5 of 326	0.0155
GO:0031090	organelle membrane	6 of 489	0.0182
GO:0044425	membrane part	8 of 844	0.0202
GO:0005741	mitochondrial outer membrane	2 of 34	0.0202
GO:0031461	cullin-RING ubiquitin ligase complex	2 of 36	0.0211
GO:0005654	nucleoplasm	3 of 140	0.0321
GO:0098805	whole membrane	3 of 154	0.0390

(less ...)

Reference publications

publication	*(year) title*	*count in gene set*	*false discovery rate*
PMID:20830285	(2010) Thyrotroph embryonic factor regulates light-induced...	4 of 22	0.0033
PMID:21390203	(2011) The light responsive transcriptome of the zebrafish: ...	5 of 75	0.0072
PMID:25079074	(2014) Redox state and mitochondrial respiratory chain fun...	3 of 17	0.0175
PMID:21756345	(2011) Cellular expression of Smarca4 (Brg1)-regulated ge...	4 of 47	0.0175
PMID:20415721	(2010) Cell resilience in species life spans: a link to inflam...	3 of 15	0.0175

(more ...)

KEGG Pathways

pathway	*description*	*count in gene set*	*false discovery rate*
dre04340	Hedgehog signaling pathway	3 of 52	0.0281

UniProt Keywords

keyword	*description*	*count in gene set*	*false discovery rate*
KW-0539	Nucleus	16 of 1851	0.0262
KW-0802	TPR repeat	4 of 114	0.0289
KW-0496	Mitochondrion	6 of 319	0.0289
KW-0677	Repeat	14 of 1754	0.0358

PFAM Protein Domains

domain	*description*	*count in gene set*	*false discovery rate*
PF13844	Glycosyl transferase family 41	2 of 2	0.0098
PF07719	Tetratricopeptide repeat	3 of 31	0.0098
PF00515	Tetratricopeptide repeat	3 of 27	0.0098
PF13431	Tetratricopeptide repeat	2 of 6	0.0113
PF13414	TPR repeat	2 of 13	0.0334

INTERPRO Protein Domains and Features

domain	*description*	*count in gene set*	*false discovery rate*
IPR001440	Tetratricopeptide repeat 1	3 of 14	0.0056
IPR037919	UDP-N-acetylglucosamine--peptide N-acetylglucosaminyltr...	2 of 2	0.0082
IPR029489	O-GlcNAc transferase, C-terminal	2 of 2	0.0082
IPR019734	Tetratricopeptide repeat	4 of 121	0.0478
IPR013026	Tetratricopeptide repeat-containing domain	4 of 121	0.0478

Statistical background

For the above enrichment analysis, the following statistical background is assumed: Whole Genome UPDATE

Save / Export

Biological Process (GO)	download	*28 GO-terms significantly enriched; file-format: tab-delimited*
Molecular Function (GO)	download	*4 GO-terms significantly enriched; file-format: tab-delimited*
Cellular Component (GO)	download	*20 GO-terms significantly enriched; file-format: tab-delimited*
Reference publications	download	*62 publications significantly enriched; file-format: tab-delimited*
KEGG Pathways	download	*one single pathway is enriched; file-format: tab-delimited*
UniProt Keywords	download	*4 keywords significantly enriched; file-format: tab-delimited*
PFAM Protein Domains	download	*5 domains significantly enriched; file-format: tab-delimited*
INTERPRO Protein Domains and Features	download	*5 domains significantly enriched; file-format: tab-delimited*

*there were **no** significant pathway enrichments observed in the following categories: Reactome Pathways, SMART Protein Domains.*

Server load: low (8%) [HD] Permalink

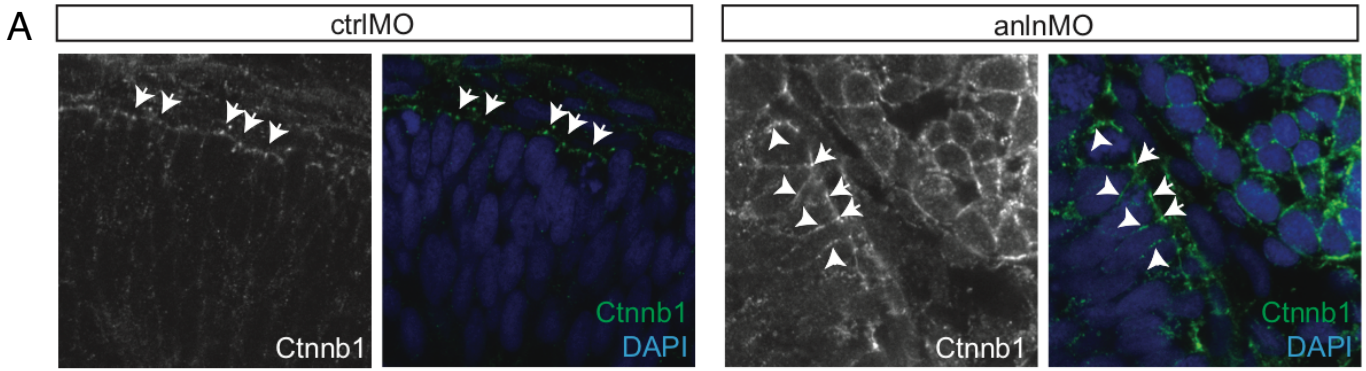

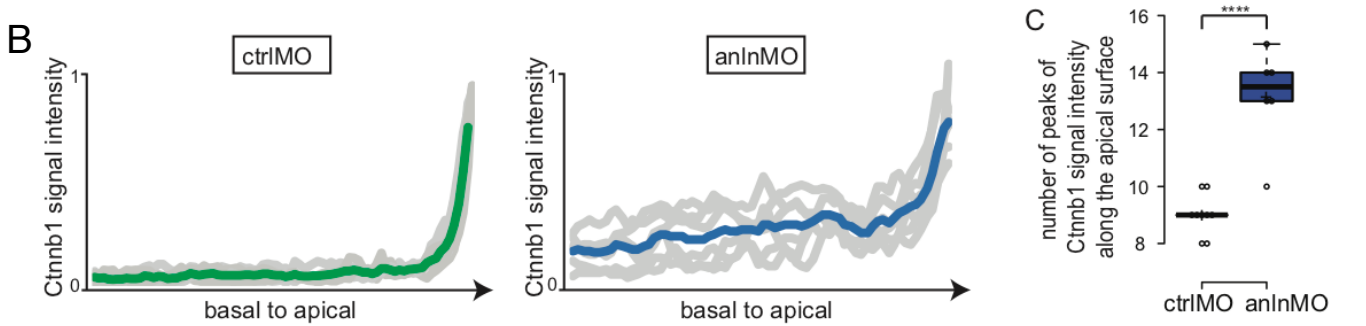

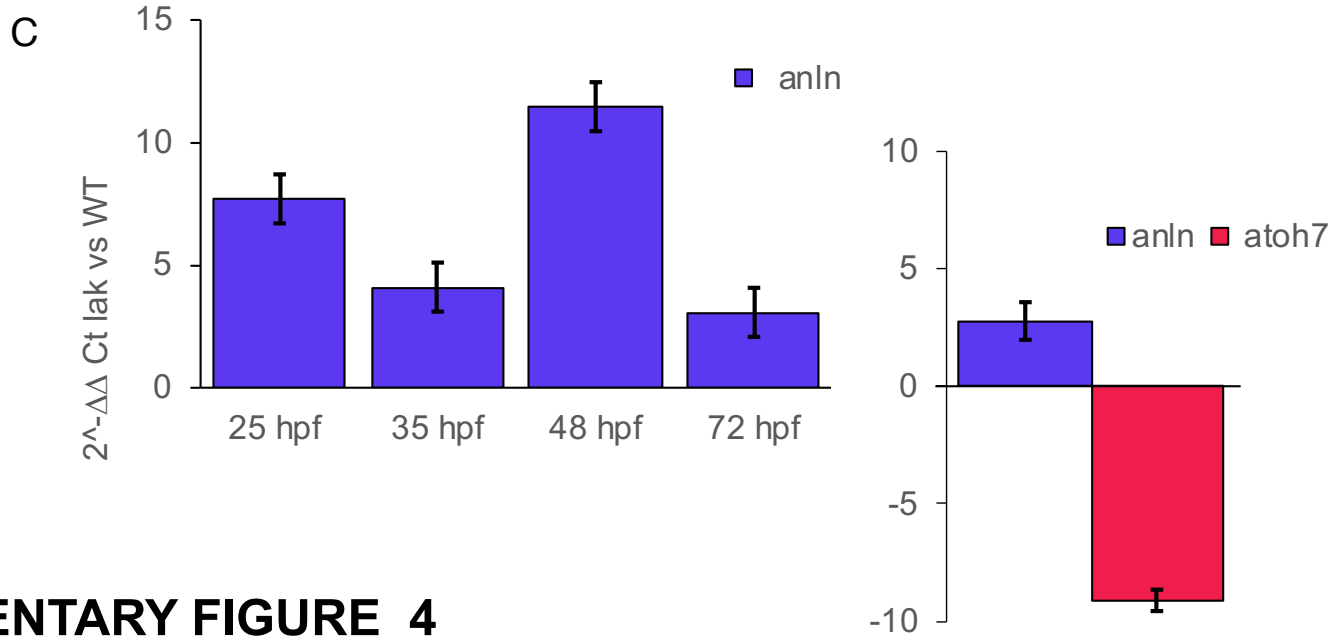

SUPPLEMENTARY FIGURE 4